

William Reix

## **Heat flux meter Calibration**

SP Technical Notes 2005:09  
Fire Technology  
Borås 2005

## Abstract

SP has developed a procedure for calibration of heat flux meters. This procedure, described in ISO/DIS 14932-2 (method 2), comprises a spherical black body cavity as a radiant heat source. The furnace has a downward-facing opening with the heat flux meter fitted in the opening in a specially designed holder. The walls of the opening, and the holder, are water-cooled. The upper part of the holder incorporates flanges that prevent radiation from being reflected onto the heat flux meter. The downward position of the furnace aperture minimises the effects of air flow or convection that could otherwise result in significant errors.

The equipment at SP has been upgraded. This report presents the results of calibrations performed in the new furnace, calculations to estimate the convective part, and a heat balance study in order to investigate the possible non-linearities in the voltage output.

Several comparisons have been carried out between heat flux meters calibrated in the old and the new furnace, and the results have been found to agree.

Key words: heat flux, heat flux meter, thermal radiation, convection, calibration.

**SP Sveriges Provnings- och  
Forskningsinstitut**  
SP AR 2005:09  
Borås 2005

**SP Swedish National Testing and  
Research Institute**  
SP Technical Notes 2005:09

Postal address:  
Box 857,  
SE-501 15 BORÅS, Sweden  
Telephone: +46 33 16 50 00  
Telex: 36252 Testing S  
Telefax: +46 33 13 55 02  
E-mail: info@sp.se

## **Acknowledgements**

First of all, I would like to thank Mrs Ingrid Wetterlund, my supervisor, for being so welcoming and helpful, in my work and my integration in Sweden.

I would want to thank especially Dr Petra Andersson and Dr Patrick Van Hees, head of the section Development and Research, for their warm welcome in Brandteknik and their kindness.

I also thank everybody at Fire Technology for being so welcoming and helpful, with a special attention to Fredrik Rosén, Tommy Hertzberg, Jesper Axelsson, Patrik Johansson, Prof Ulf Wickström, head of the Fire Technology department, Joel Blom, and Erika Hjelm.

At last, I would like to thank Mr René Cavel and Mlle Nashida Bourabaa, my teachers in Valenciennes University.

# Contents

	<b>Abstract</b>	<b>2</b>
	<b>Acknowledgements</b>	<b>3</b>
	<b>Nomenclature</b>	<b>6</b>
<b>1</b>	<b>Introduction</b>	<b>7</b>
<b>2</b>	<b>Work programme</b>	<b>8</b>
2.1	Calibrations in the new furnace and comparisons with the old one	8
2.2	Calibrations where the heat flux meter is mounted flush with the wall	8
2.3	Calculations to estimate the convective part	8
2.4	Studying the heat balance in the heat flux meter and especially investigating possible non-linearities	8
<b>3</b>	<b>Heat flux meters</b>	<b>9</b>
3.1	Description of Gardon Gauge	9
3.2	Description of Schmidt Boelter Gauge	10
<b>4</b>	<b>Calibration of heat flux meters</b>	<b>11</b>
4.1	Operating procedure	11
4.2	The spherical furnace chamber	12
4.3	The cooler and its insert	13
<b>5</b>	<b>Parameters influencing the heat flux calculation</b>	<b>15</b>
5.1	Dimension measurements	15
5.2	Measurements of temperatures in the furnace	16
5.2.1	Pyrometer measurement	16
5.2.2	Measurements with movable thermocouple	17
5.3	Measurements of temperatures in the cooler	18
5.4	Emissivities	18
5.4.1	Values of $\epsilon_1$ , $\epsilon_2$ , $\epsilon_3$ , $\epsilon_4$ and $\epsilon_5$ .	18
5.4.2	Influence of black painted cooler	19
5.4.3	Wavelength	19
<b>6</b>	<b>Comparisons</b>	<b>21</b>
<b>7</b>	<b>Calibration flush with the wall</b>	<b>22</b>
<b>8</b>	<b>Convective contribution in the SP furnace</b>	<b>25</b>
8.1	Heat balance on the gauge	25
8.2	Determination of the convective part	26
8.3	1 <sup>st</sup> Method – Heat balance	26
8.3.1	Assumptions	27
8.3.2	Results	27
8.3.3	Uncertainties in the model	27
8.4	2 <sup>nd</sup> Method - Calculation with femlab	27
8.5	3 <sup>rd</sup> Method– Direct method using the of air flow velocity	31
8.5.1	Calculation of ambient temperature $T_a$	32
8.5.2	Measurement of ambient temperature $T_a$	33
8.5.3	Calculation of the heat transfer coefficient h	33

<b>9</b>	<b>Investigation of possible non-linearities in the calibration</b>	<b>35</b>
9.1	Heat balance on the gauge	35
9.2	Simplification of the calibration	37
<b>10</b>	<b>Conclusion</b>	<b>39</b>
<b>11</b>	<b>References</b>	<b>40</b>
	<b>Annex A Theory of the calculation</b>	<b>41</b>
	<b>Annex B Results of the calibrations using standard procedure</b>	<b>50</b>
	<b>Annex C Results of the comparisons</b>	<b>58</b>
	<b>Annex D One point calibration</b>	<b>60</b>
	<b>Annex E Results of the calibrations, HFM flush with the wall</b>	<b>62</b>
	<b>Annex F Table thermocouple T</b>	<b>66</b>

## Nomenclature

$T_a$	Temperature of air next to the sensor ( $K$ )
$T_s$	Temperature at the surface of the sensor ( $K$ )
$T_w$	Water temperature ( $K$ )
$T_f$	Furnace temperature ( $K$ )
$T_{film}$	Film temperature ( $K$ )
$T_i$	temperature of area i
$T_{up}$	Temperature of the upper junction of the thermopile
$T_{low}$	Temperature of the lower junction of the thermopile
$q_i$	Net radiation per unit area leaving area i ( $W \cdot m^{-2}$ )
$q$	Heat flux ( $W \cdot m^{-2}$ )
$\sigma$	Stefan-Boltzmann's constant ( $5,67 \cdot 10^{-8} W / K^4 m^2$ )
$e_{bi}$	Black body radiation( $\sigma T_f^4$ ) leaving area i ( $W \cdot m^{-2}$ )
$\epsilon_i$	Emissivity of the area i (dimensionless number)
$\epsilon$	Emissivity of the sensor (dimensionless number)
$h$	Heat transfer coefficient ( $W \cdot m^{-2} K^{-1}$ )
$\phi$	Configuration factor ( dimensionless number)
$\delta$	Thickness of the thermopile ( $m$ )
$X$	Characteristic length ( $m$ )
$D$	Diameter of the spherical chamber (m)
$d_1$	diameter of the aperture (m)
$d$	diameter of the sensor
$k$	Thermal conductivity ( $W \cdot m^{-1} \cdot K^{-1}$ )
$k_{air}$	Thermal conductivity of air ( $W \cdot m^{-1} K^{-1}$ )
$C_p$	Heat capacity ( $kJ \cdot kg^{-1} \cdot ^\circ C^{-1}$ )
$\rho$	density ( $kg \cdot m^{-3}$ )
$\alpha$	Thermal diffusivity ( $m^2 \cdot s^{-1}$ )
$\nu$	Kinematic viscosity of air ( $m^2 \cdot s^{-1}$ )
$u$	Output voltage (mV )
$V$	Velocity of air close to the sensor ( $m \cdot s^{-1}$ )
$Pr$	Prandtl Number calculated at $T_{film}$ (dimensionless number)
$Re$	Reynolds Number (dimensionless number)
$g$	Gravity acceleration ( $m^2 \cdot s^{-2}$ )
$N$	Number of junction in a thermocouple

# 1 Introduction

Measurements of heat flux are often required in standard fire testing to set up the apparatus for the test. It is also used in fire research experiments to measure the thermal impact on targets. It is important to be able to calibrate the heat flux meters used for setting up standard fire tests and research purposes with an adequate uncertainty.

Currently a number of procedures are used internationally. These procedures are described in a series of standards with the number ISO 14934 and the general title *Fire tests — Calibration and use of heat flux meters*. The series consists of four parts:

- *Part 1: General principles* [1]
- *Part 2: Primary calibration methods* [2]
- *Part 3: Secondary calibration methods* [3]
- *Part 4: Guidance on the use of heat flux meters in fire tests* [4]

The investigations performed in this project aim to make the procedures of ISO 14934 internationally more accepted. The work is part of the project no 04153 from Nordic Innovation Centre. The work comprises development of a calibration scheme for heat flux meters.

To calibrate heat flux meters, SP uses a spherical black-body method. The method is described in ISO/DIS 14934-2 [1]. The equipment consists of a well-insulated, electrically heated spherical furnace chamber.

SP has used a spherical furnace for more than 10 years. The old furnace had a water cooled bottom in addition to the water cooled aperture. The connection between the bottom cooler and the aperture cooler gradually deteriorated and water started to leak out. Although the leakage was repaired several times, the reparations finally were unsuccessful and the furnace could no longer be used. The furnace was therefore replaced in January 2005.

The new furnace with the model no M350 has the same design with respect to the calibration principle as the old one. It was built by Mikron Infrared, Inc in Oakland, New Jersey, USA.

The work on evaluating the performance of the new furnace is reported here.

## **2 Work programme**

The work programme consists of the following parts:

- Calibrations in the new furnace and comparisons with the old one
- Calibrations where the heat flux meter is mounted flush with the wall
- Calculations to estimate the convective part
- Studying the heat balance in the heat flux meter and especially investigating possible non-linearities

### **2.1 Calibrations in the new furnace and comparisons with the old one**

It was of paramount importance to test the new furnace and make as many calibrations as possible to make sure that the new equipment was working well. The results obtained with the former furnace were good, as shown by comparisons made with the other institutes [5]. Thus all the results obtained with the new furnace have been compared with those obtained with the former one. The work is presented in chapter 6.

### **2.2 Calibrations where the heat flux meter is mounted flush with the wall**

The plans of the NICE project 04153 includes to work out a simpler procedure. Therefore a procedure similar to the one used at SINTEF-NBL in Norway, i.e. to mount the heat flux meters flush with the wall, was investigated. The work is presented in chapter 7.

### **2.3 Calculations to estimate the convective part**

Heat can be transmitted by three modes: convection, conduction, and radiation. The aim of the calibration method used is to find a relationship between the irradiation (net radiative heat flux) to the gauge, and the output voltage which is measured. The problem is that the HFM are not only responding to radiation, but can have responses that are sensitive to all modes. Depending on how the gage is installed, surrounding structure and aerothermal environment can cause unexpected convection which can disturb the results. Therefore should the convective part be evaluated in the total heat flux calculation. The work is presented in chapter 8.

### **2.4 Studying the heat balance in the heat flux meter and especially investigating possible non-linearities**

It is often assumed that the output voltage measured is proportional to the heat flux received by the sensor. This assumption has been checked in two ways: practically, by analysing the curves obtained, and theoretically by setting up the heat balance on the gauges. If this assumption is valid, the calibration procedure could be simplified. The work is presented in chapter 9.

### 3 Heat flux meters

Radiant heat flux is usually measured with a heat flux meter (HFM). The heat flux meter gives an output voltage signal that depends on the temperature of the sensing area. This temperature depends on the incident radiation or rather heat flux. There are two different types of HFM available, the Gardon gauge and the Schmidt-Boelter gauge. Both types sense the total heat flux that impinges on the receiving surface. Thus, the gauges are not only responding to radiation, but also to convection. That fact imposes certain problems when the gauges are used to measure radiation only.

#### 3.1 Gardon Gauge

The Gardon gauge, as described in Figure 3-1 is operating with a radially distributed heat flow over its sensitive surface.

The sensor disk is made of constantan (a copper-nickel alloy, 55% copper and 45% nickel) and is attached to a copper lead to form a single thermocouple T. As the disk is cooled only at its periphery, it develops a comparably high centre temperature. The radial temperature distribution is therefore rather non-uniform, with a peak at the centre of the disk.

The copper body usually has a diameter of 2.5 cm, and the sensor disk has a diameter ranging between 3 and 6 mm.

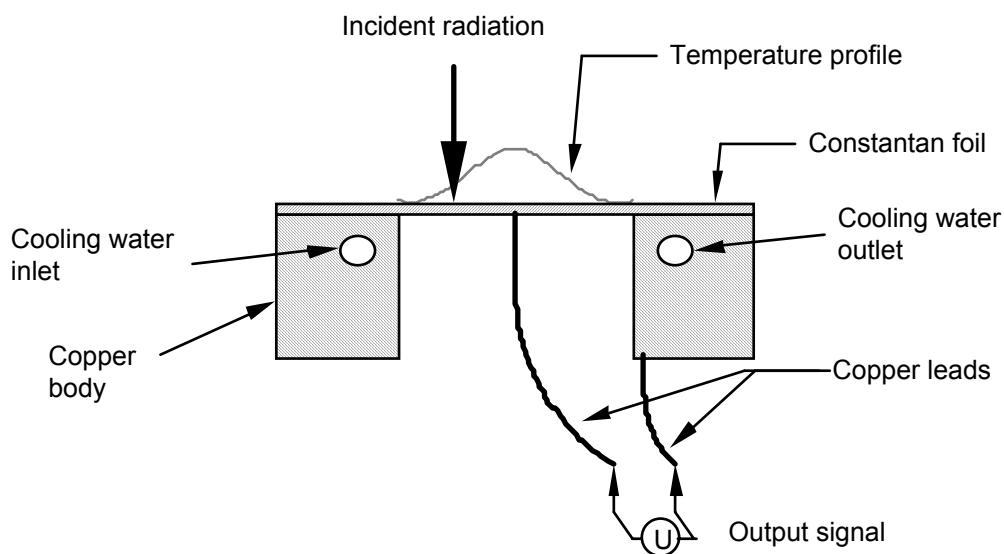
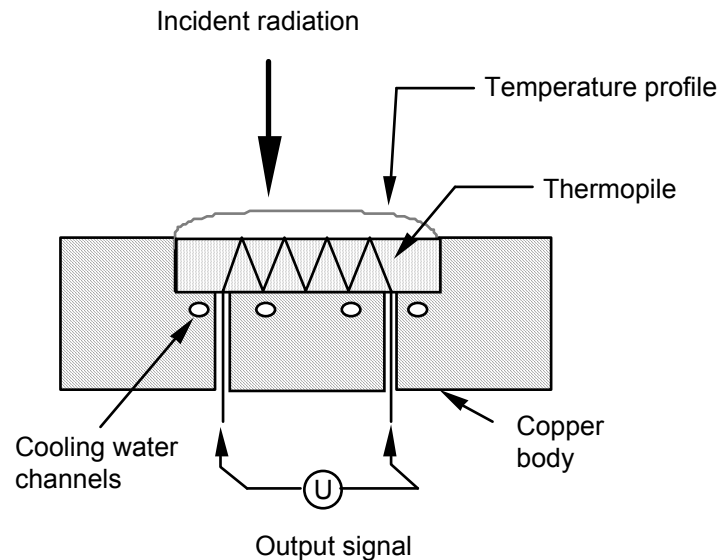


Figure 3-1 Schematic drawing of a Gardon gage and some of its basic parameters. Cross-section (not in scale).

## 3.2 Schmidt Boelter Gauge

The second type, called the Schmidt-Boelter gauge (SB gauge), operates on the basis of an axially heat flow, i.e. perpendicular to the receiving surface. The principle is depicted in Figure 3-2.



**Figure 3-2** Schematic drawing of a Schmidt-Boelter gage and some basic parameters. Cross-section (not in scale).

The sensing element is here a thermopile, with a varying number of junctions. The number of junctions depends on the range of heat flux which the gauge is designed to measure.

As the receiving disk is cooled both radially and axially, it does not develop such a high centre temperature as the Gardon gauge. The temperature profile over the disk is consequently more uniform.

The dimensions of the copper body and the sensor disk are of the same order as those of the Gardon gauge.

## 4 Calibration of heat flux meters

The calibration procedure used at SP is based on the use of a spherical furnace chamber, which is well insulated and electrically heated. The method was developed by Sören Olsson [6] and is also well described in ISO/DIS 14934-2 [2].

The furnace is considered as a black body radiant heat source. A cooling device, housing the HFM that is to be calibrated, is inserted in an opening in the bottom of the furnace. The sensing surface of the heat flux meter is oriented horizontally, and the HFM is inserted at the bottom of the furnace. Thus the influence of convection is reduced to a minimum. The aperture in the cooling device defines the view factor under which the furnace radiates to the heat flux.

When the temperature of the blackbody has stabilized, records of the water and the furnace temperature together with the output signal from the gauge are taken. The heat flux is deduced using a calculation procedure. The deduction is repeated for each furnace temperature. The heat flux towards output voltage is then plotted.

### 4.1 Operating procedure

The different steps of the calibration procedure are:

- a) Identify the heat flux meter.  
Manufacturer, type, serial number, and maximum allowable radiation in  $\text{kW/m}^2$ .
- b) Decide which 10 radiation levels the heat flux meter is going to be calibrated at. Enter the temperatures corresponding to each radiation level in the protocol. Determine if a spacer ring has to be used. The radiation can be varied between 6 and 75  $\text{kW/m}^2$  without the spacer ring, and between 2 and 25  $\text{kW/m}^2$  with the ring.
- c) Measure radius  $r_5$  of the heat flux meter's receiving sensor.
- d) Insert the HFM in the holder (the movable cooler) using the appropriate fixture and secure its position with the locking screws.
- e) Carefully measure the depth  $X_g$  of the heat flux meter carefully, (distance between top of movable cooler and heat flux meter's receiving sensor) with a 0,01 mm depth gage.
- f) Connect all measuring devices to the computer.
- g) Connect water supply to the cooling system of the holder and the HFM.
- h) Insert the holder in the sight tube and secure with lock nuts. Don't forget to put the spacer on the top of holder if it's needed.
- i) Connect the electric wire to the wire that goes to the computer.
- j) Switch on the furnace. The "water-off-alarm" will sound.
- k) Turn the water on. The setting for the HFM should be about 20. The setting on the other two flows should be max opened. Control that the water temperature is at 25°C.

- l) Set the first set point temperature according to the protocol.
- m) Allow the temperature to stabilize. The temperature on the controller display should show the same value as the set-point, to the decimal.
- n) Start the measuring and take the record during 2 minutes (approx 120 readings). Be sure that the temperature is stable.
- o) Repeat l-n for next level of radiation.

## 4.2 The spherical furnace chamber

The spherical blackbody cavity, represented schematically in Figure 4-1, is a 300 mm diameter spherical furnace fitted with a 60.18 mm diameter aperture. The spherical furnace wall is made of inconel. On the outside of that shell, evenly distributed electrical heating coils are attached with a ceramic compound with good thermal conductivity. The furnace chamber is embedded in high temperature resistant ceramic insulation to minimize heat losses and establish an even temperature distribution.

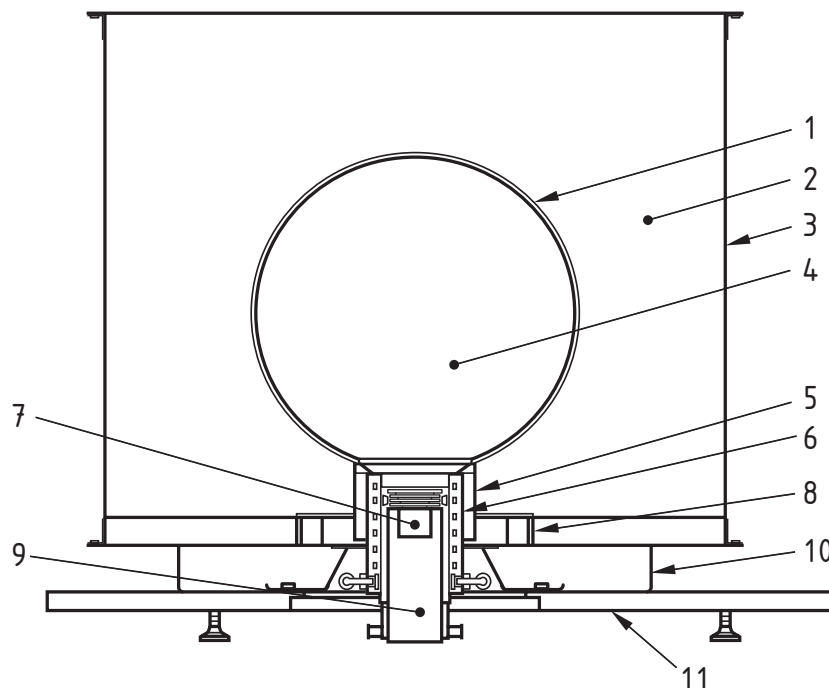


**Figure 4-1** Schematic picture of the furnace, orientated with the hole for the cooler at the bottom (vertical cross-section). The movable cooler inserts is shown with a gage fitted

Key:

- |  |   |
|--|---|
| 1 Spherical cavity with heater in ceramic casting  | 7 Heat flux meter                               |
| 2 Low density ceramic insulation                   | 8 Ceramic insulator stand-offs                  |
| 3 Interior stainless steel housing                 | 9 Movable, water cooled, heat flux meter holder |
| 4 Thermocouple attached to sphere interior surface | 10 Interior support structure                   |
| 5 Hard ceramic insulator                           | 11 Bottom face plate                            |
| 6 Water cooled sight tube                          |   |

### 4.3 The cooler and its insert

As described by Olsson [6] the cooler consists of an assembly of concentric cylinders, with a system of water channels in between. The cooling water temperature must be higher than the dewpoint of the ambient air, in order to avoid condensation of air humidity on the cooler and the gauge. For the gauge itself and its operation, the temperature of the cooling water does not matter too much, but the accuracy of the calibration will be better the lower the water temperature. A water temperature of 25 °C was therefore chosen to perform all normal calibrations as this will be over the dewpoint in most situations.

The inner part of the fixed cooler is carefully machined to accurate dimensions. Its top opening forms an aperture, through which the furnace radiates to the heat flux meter. Some distance down ( $X_1$ ) a flange is located. This flange serves partly as a stray radiation shield, but mainly as a rest, in order to position the water cooled heat flux meter holder exactly.

The cooler is designed for use with the heat flux meter holder (a movable insert) in two positions: The top position and a position 40 mm below that provides for radiation ranges of 6-75 kW/m<sup>2</sup> and 2-25 kW/m<sup>2</sup> respectively at the temperature interval 400-1000 °C. To set the movable insert in its lowest position, a spacer ring is used. Figure 4-2 shows the heat flux meter holder in its top position.

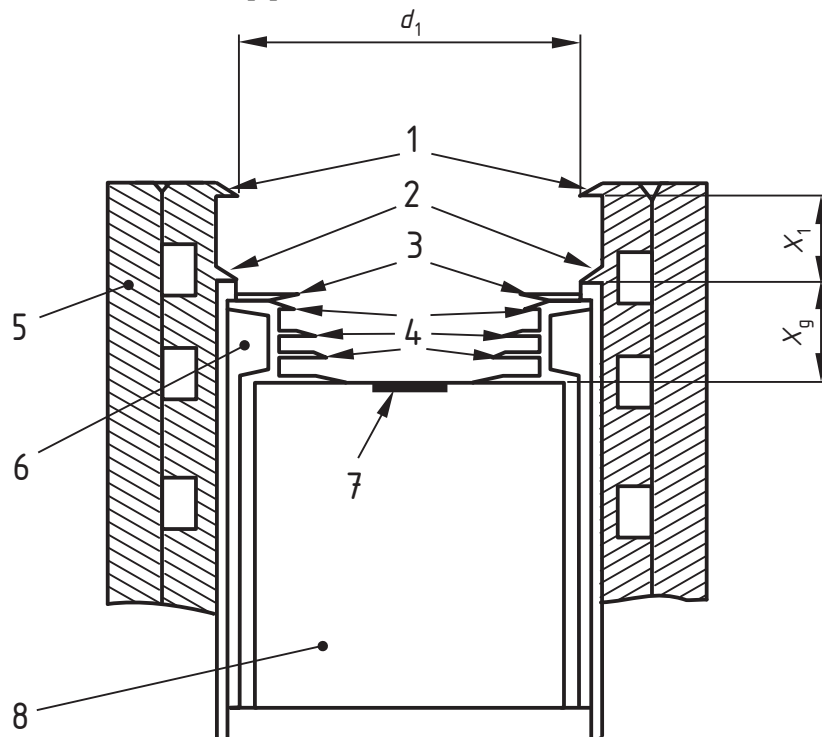


Figure 4-2 The inner part of the cooler system with the movable part in its top position.

Key:

- |  |  |
|--|--|
| 1 Restricting aperture                                       | 5 Inner part of sight tube with water channels |
| 2 Upper shielding flange and rest for heat flux meter holder | 6 Heat flux meter holder with water channels   |
| 3 Aperture disc  | 7 Sensing surface                              |
| 4 Shielding flanges of heat flux meter holder                | 8 Heat flux meter body (schematic)             |

The holder has a number of flanges which protect the heat flux meter from receiving radiation reflected from the cooled holder wall. The flanges also help to conserve the stratification of air, which reduces convective heat transfer to the heat flux meter sensing surface.

Figure 4-3 shows the heat flux meter holder in its position 40 mm below, with the spacer ring inserted, but otherwise identical.

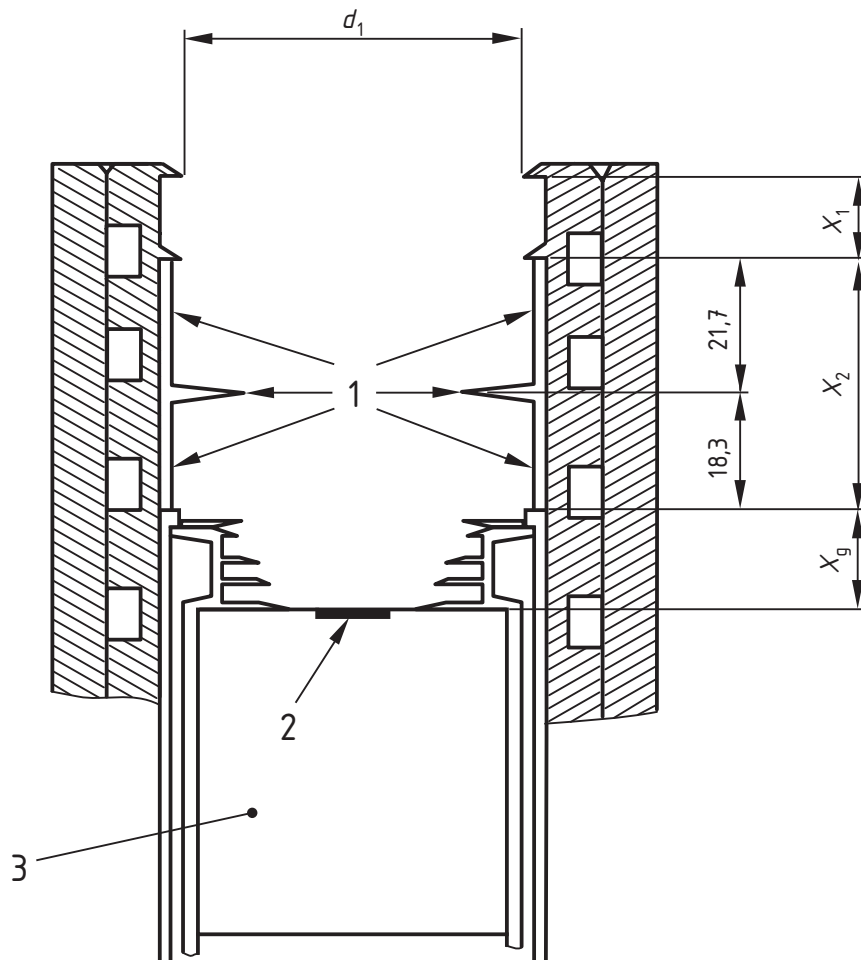


**Figure 4-3** The inner part of the cooler system with the movable part 40.05 mm below the top position and with the spacer ring inserted. The distance  $X_2$  is  $40.05 \pm 0.02$  mm.

Key:

- |   |                                   |   |                                  |
|---|-----------------------------------|---|----------------------------------|
| 1 | Spacer ring with shielding flange | 3 | Heat flux meter body (schematic) |
| 2 | Sensing surface                   |   |                                  |

Inside the removable spacer ring there is another flange for shielding of reflection. The spacer also serves to ensure exact positioning of the holder in its lowest position.

The aperture diameter  $d_1$  is  $(60,18 \pm 0,01)$  mm and the distance  $X_1$  is  $(13,05 \pm 0,03)$  mm. Note that the distance  $X_g$  will vary, depending on the heat flux meter design, as it is the distance between the top of the holder and the sensing surface of the heat flux meter. Normally it is around 17 mm.

## 5 Parameters influencing the heat flux calculation

Parameters studied in this project that are included in the heat flux calculation are presented below. A complete list of parameters included in the heat flux calculation is given in Olsson's report [6].

### 5.1 Dimension measurements

Some of the dimensions of the movable cooler and of the fitting piece were measured to confirm calculation of the view factors. A slide calliper with 2 decimal digits and a depth gauge were used. Both instruments were calibrated with an uncertainty of 0,03 mm. The measured dimensions are given in Figure 5-1 and the results of the measurements in Table 5-1.

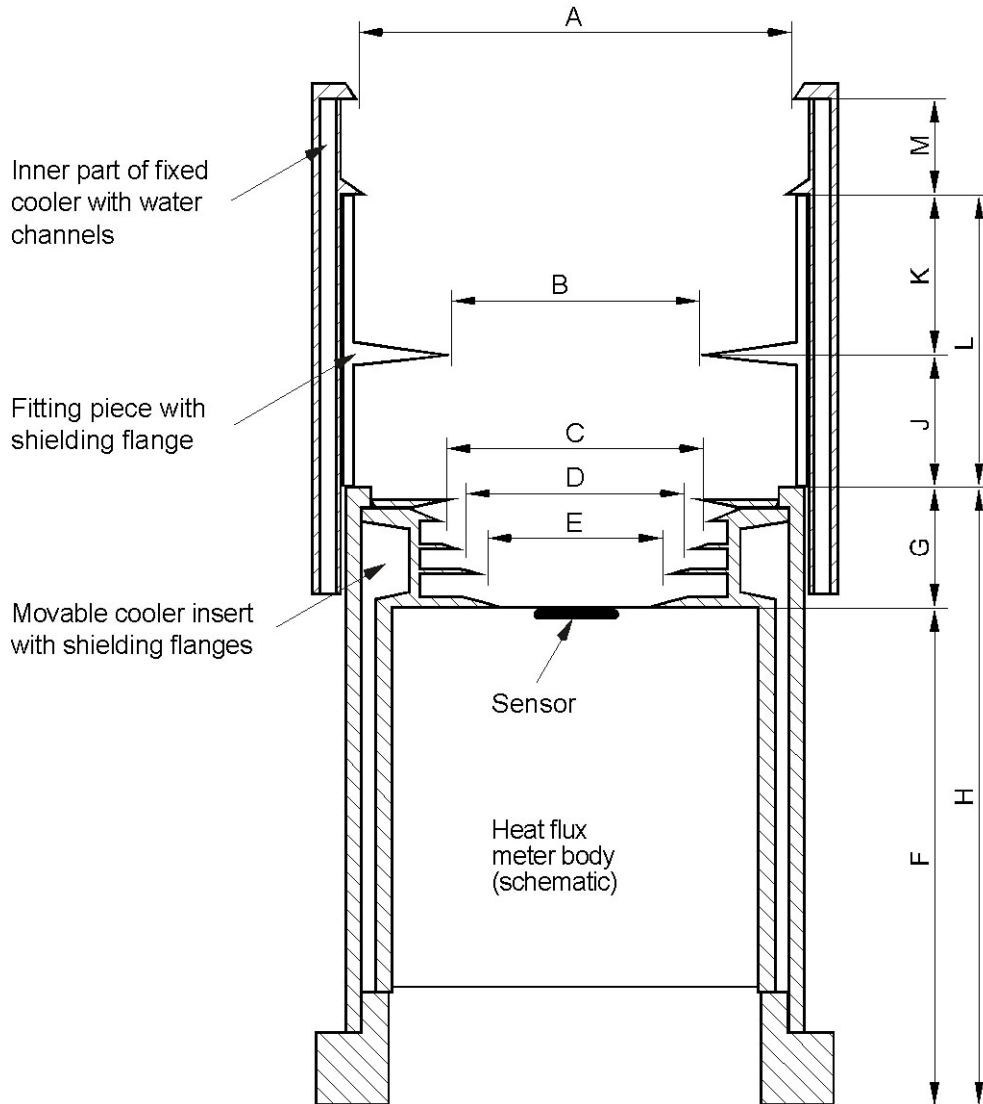


**Figure 5-1** Controlled dimensions of fixed and movable cooler. (With respect to the construction of the cooling system of the fixed cooler this figure reflects the old furnace. All flanges are equally designed in both furnaces)

**Table 5-1 Results of control of dimensions of fixed and movable cooler**

Dimension identification	Dimensions (mm) according to Mikron Manual	Measured dimensions (mm)
A		60.18
B	35.0	36.99
C	37.0	36.99
D	32.0	32.01
E	27.0	27.03
F		
G	<sup>1)</sup>	<sup>1)</sup>
H	148.0	
J	18.3	18.54
K	21.7	21.96
L	40.0	40.05
M		13.06

- <sup>1)</sup> G (called  $X_g$ ) depends of both the heat flux meter design and how the screws which maintain the HFM in the holder are tightened. This measure has to be taken each time a calibration is performed.

## 5.2 Measurements of temperatures in the furnace

The most essential parameter to determine the heat flux received by the sensor is the furnace temperature. The temperature in the furnace is not uniform. This makes it difficult to measure the temperature used for radiation calculation. Therefore one need to decide which temperature reflects best the radiation. Two different ways were used to determine this temperature. The first was to compare the values used for the calculation, and the values measured by pyrometers. The second way was to insert a movable thermocouple inside the furnace, and measure the temperature at different positions.

### 5.2.1 Pyrometer measurement

Measurements were done with two pyrometers. The pyrometers were held about one meter below the outer opening of the sight tube. The target was that part of the furnace wall which is visible from this distance. The line of sight was aligned with the central axis of the sight tube. The measurements were repeated three times.

The results are shown in Table 5-2 below. In this table, TC 2 is the temperature measured by the thermocouple inside the furnace. It is this temperature which is used in the calculation. M190 Q and C52 are the references of two different pyrometers. All temperatures are in °C.

**Table 5-2 Measurements of the furnace temperatures with the pyrometers. Temperature in °C**

Reference	TC2					
	1st measure	2nd measure	3rd measure			
1000	981.6	981.3	981.4			
900	885.8	885.8	885.5			
800	788.4	788.2	788.0			
700	690.7	690.6	690.6			
600	591.7	591.4	591.4			
500	491.6	491.6	491.4			
400	392.0	392.0	391.8			
Reference	M190Q			C52		
	1st measure	2nd measure	3rd measure	1st measure	2nd measure	3rd measure
1000	990.0	987.1	990.4	989.0	991.5	990.5
900	891.9	887.8	890.7	891.6	892.1	892.1
800	795.1	791.3	794.7	794.7	794.7	794.7
700	696.8	696.1	697.1	697.2	697.2	697.2
600	597.4	597.0	597.1	597.6	597.6	597.6
500	497.0	494.9	496.5			
400	397.7	397.7	397.5			

As can be seen in the table, the temperatures measured by the pyrometers are approximately equal to each other and about 5% higher than those obtained by the thermocouple.

## 5.2.2 Measurements with movable thermocouple

A thermocouple was inserted in the furnace by the outer opening of the sight tube. The measurements were done at a reference temperature of 500°C, and were taken for several distances from the wall of the furnace. The results are presented in Table 5-3 below. All temperatures are in °C.

**Table 5-3 Measurements of the furnace temperatures at different distances from the wall**

distance from the wall	TC 2	movable thermocouple
0.2 cm	491.3	496.5
2 cm	491.3	495.9
4 cm	491.3	495.1
6 cm	491.3	494.2
8 cm	491.2	493.1
10 cm	491.1	492.0
12 cm	491.2	490.8
14 cm	491.1	489.4
19 cm	491.6	486.2

As can be seen, the temperature decreases towards and below the centre of the furnace (which has a diameter of 300 mm). The difference between the temperature close to the surface of the wall (0.2 cm) and in the centre of the furnace is about 2%.

A temperature difference of 2% is equal to a heat flux difference of 5-6%.

### 5.3 Measurements of temperatures in the cooler

The temperatures in the cooler are also parameters useful to know accurately to calculate the heat flux.

A series of separate experiments were performed by Olsson [6], in which the temperature of the inner surface of the cooler was measured at various locations, as shown in Figure 5-2. Since no measurements were done in this project Olsson's data have been used.

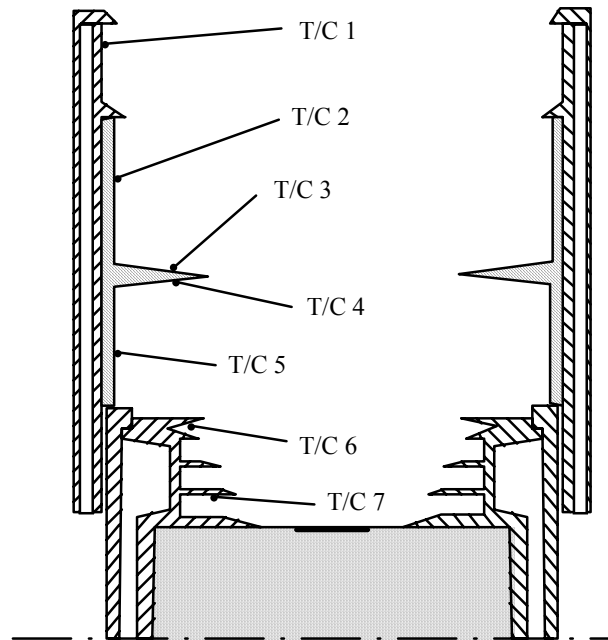


Figure 5-2 Cross-section of the cooler, with locations of the thermocouples used in the experiments. (Figure from Olsson's report [6])

The results of these measurements are presented in the Olsson report [6].

### 5.4 Emissivities

#### 5.4.1 Values of $\epsilon_1$ , $\epsilon_2$ , $\epsilon_3$ , $\epsilon_4$ and $\epsilon_5$ .

According to Olsson's report [6], the emissivities  $\epsilon_2$ ,  $\epsilon_3$  and  $\epsilon_4$  are equal to 0.96. The emissivity of the sensor,  $\epsilon_5$ , is set to be 1. The apparent emissivity of the furnace,  $\epsilon_1$ , is calculated according to the formulae below:

$$\epsilon_1 = \frac{1}{1 + \frac{d_1^2}{4D^2} \frac{1 - \epsilon_f}{\epsilon_f}} \quad (5-1)$$

Where  $D$  = the diameter of the spherical chamber (m)  
 $d_1$  = the diameter of the aperture (m)  
 $\epsilon_f$  = the emissivity of the furnace wall

With the values of  $D = 300$  mm,  $d_1 = 60.18$  mm and  $\epsilon_f = 0.8$  (mean values), this expression gives an apparent emissivity of 0.997 which has been used in the calculations.

### 5.4.2 Influence of black painted cooler

In order to investigate the influence of blackening the cooler two calibrations were performed, one before the cooler was painted, and one after it was painted. The painting was done with matt black spray paint. Figure 5-3 shows the result for calibrations performed with HFM 700263 before and after the cooler was painted black. The spacer ring was used at the calibration.

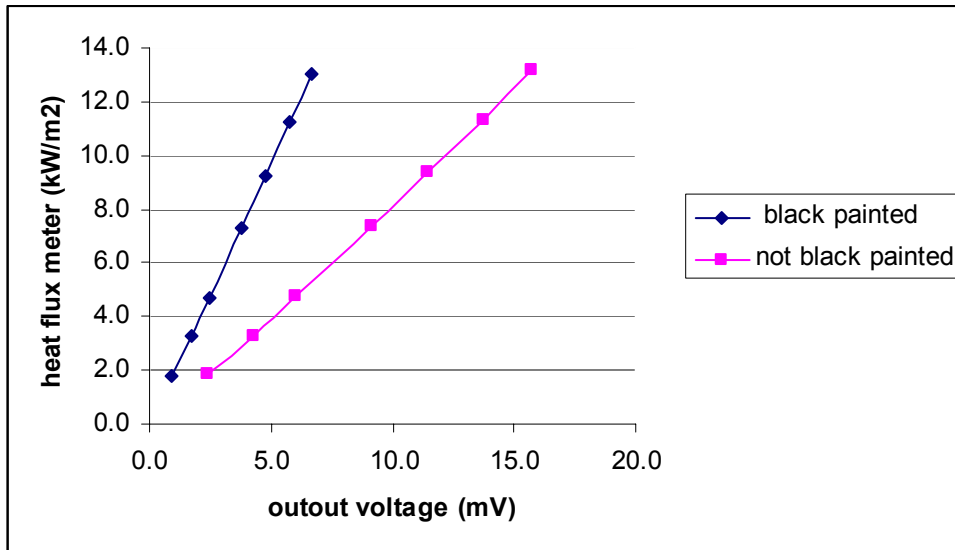


Figure 5-3 Influence of blackening the cooler

The difference between the two curves is 95.8%! For a calibration without the spacer ring, the difference was approximately 25%.

These differences could be explained by the fact that if the holder is not painted, the surfaces reflect more. The reflected heat adds to the initial heat and for the same heat flux the voltage output thus becomes higher. This difference is of course more important when the spacer ring is used since the surface that is not painted is larger in this case.

### 5.4.3 Wavelength

The emissivities of various substances vary widely with wavelength, temperature, and surface condition. The functional relation for  $E_{b\lambda}$ , the emissive power of a black body per unit wavelength, was derived by Planck

$$E_{b\lambda} = \frac{C_1 \lambda^{-5}}{e^{C_2/\lambda T} - 1} \quad (5-2)$$

Where  $\lambda$  = wavelength,  $\mu\text{m}$

$T$  = temperature, K

$C_1 = 3.743 \times 10^8 \text{ W } \mu\text{m}^4/\text{m}^2$

$C_2 = 1.4387 \times 10^4 \mu\text{m K}$

The quantity of interest with regard to the blackbody emissive spectrum is the wavelength  $\lambda_{\max}$  at which the emissive power is a maximum for a given temperature. The solution to the equation (5-6) for  $\lambda_{\max}T$  is a constant, and is related by Wien's displacement law,

$$\lambda_{\max} T = 2897.6 \mu\text{m K} \quad (5-3)$$

The temperatures at which the heat flux meters are calibrated vary between 160 °C and 1000 °C. The values of  $\lambda_{\max}$  for different values of temperature have been calculated.

**Table 5-4** Calculations of  $\lambda_{\max}$

temperatures (°C)	$\lambda_{\max}$ ( $\mu\text{m}$ )
160	6.69
300	5.06
400	4.31
500	3.75
600	3.32
700	2.98
800	2.70
900	2.47
1000	2.28

From this table, it can be deduced that if the sensor was a perfect blackbody, the maximum wavelength would vary between 2.3  $\mu\text{m}$  and 6.7  $\mu\text{m}$ .

Values of emissivities of the sensor black coating have been measured in a previous work [5]. The measurements have been performed for 5 possible angles of incidence, a large range of temperature, and the spectral range of measurement was 0.8  $\mu\text{m}$  to 14  $\mu\text{m}$ . The results show that for this variation of wavelength, the emissivity of the black coating is nearly stable, varying between 0.95 and 0.98.

Therefore, the large range of temperature used for the heat flux meter calibration does not influence the emissivity. The emissivity of the sensor is set to be 1.

## 6 Comparisons

A number of heat flux meters were used to confirm the calibration results of the new furnace compared to the old one. The heat flux meters which have been calibrated are:

- HFM 123731 (Gordon gage, diameter 25,4 mm, range 100 kW/m<sup>2</sup>)
- HFM 123732 (Schmidt-Boelter gage, diameter 12,7 mm, range 100 kW/m<sup>2</sup>)
- HFM 700195 (Schmidt-Boelter gage, diameter 25,4 mm, range 20 kW/m<sup>2</sup>)
- HFM 700237 (Schmidt-Boelter gage, diameter 25,4 mm, range 20 kW/m<sup>2</sup>)
- HFM 700263 (Schmidt-Boelter gage, with spacer ring, diameter 25,4 mm, range 20 kW/m<sup>2</sup>)
- HFM 700385 (Schmidt-Boelter gage, diameter 25,4 mm, range 50 kW/m<sup>2</sup>)
- HFM 701105 (Schmidt-Boelter gage, diameter 25,4 mm, range 50 kW/m<sup>2</sup>)

HFM 123731 (G) and 123732 (SB) were borrowed from NIST in the USA. These two gauges were used in a round robin between five laboratories organised by the FORUM Heat Flux Measurement Working Group 2002. The SP results for HFM 123732 (SB) were at the median at that activity. The results for HFM 123731 (G) were slightly below median.

The detailed results of the calibrations performed in the new furnace with the above listed gauges are given in Annex B.

The calibrations performed this year with the new furnace were also compared with the calibrations performed with the old furnace. Calibration results from the manufacturer of the heat flux meters, Medtherm, are included in the comparison in some of the cases. To compare the results, the heat flux was calculated at  $u=10\text{mv}$ . The results are given in Annex C.

The average difference between the two furnaces, in term of heat flux, is approximately 1%. A difference of 1% in term of heat flux corresponds to a difference in term of temperature of about 0.3-0.4%. This correction could be made on further work.

## 7 Calibration flush with the wall

The plans of the NICE project 04153 includes the development of a simpler calibration procedure. Therefore a procedure similar to the one used at SINTEF-NBL in Norway, i.e. to mount the heat flux meters flush with the wall, was investigated. This procedure was compared to the standard procedure described in chapter 4.

Two heat flux meters from NIST were calibrated: the HFM 123731 (Gardon gauge, 1 inch) and the HFM 123732 (Schmidt-Boelter gauge, 0.5 inch). Two SP gauges were also calibrated, the HFM 700263 (SB), and the HFM 701105 (SB).

When mounted flush with the furnace wall, the heat flux meter sees all the radiation emitted by the furnace. A schematic figure of the mounting is shown in Figure 7-1.

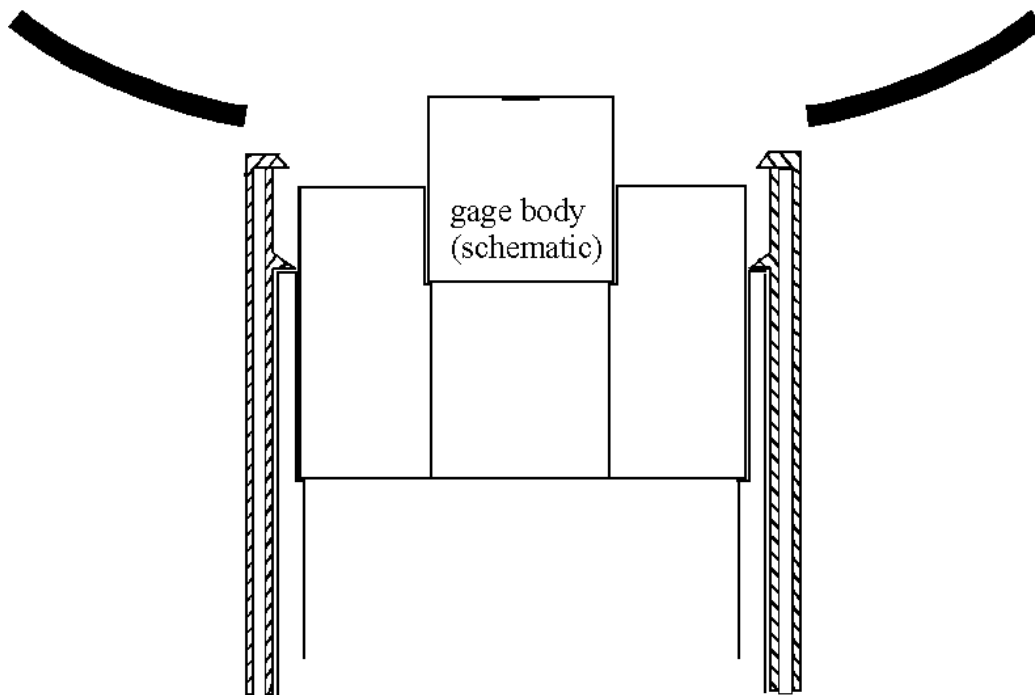


**Figure 7-1 The gauge mounted ‘flush with the wall’**

Several calibrations were performed to evaluate the mounting techniques for heat flux meter flush with the wall. The system designed to maintain the 1 inch gauges 123731 (G) and 701105 (SB) could be water cooled, but it’s not the case for the 0.5 inch HFM 123732 (SB) or for the HFM 700263 (SB) with flanges. Therefore only the HFM 123731 (G) was calibrated with all four configurations: with and without the cooling system, and with and without insulation on top of the cooled or non-cooled holder. The insulation used was Kaowool with a density of app. 280 kg/m<sup>2</sup>. The four mounting holder configurations are shown in the photos in Figure 7-2.

As a resume, these are the configurations for the calibration of HFM 123731 (G):

- With cooler, without insulation, see top left photo in Figure 7-2
- With cooler, with insulation, see top right photo in Figure 7-2
- Without cooler, without insulation, see bottom left photo in Figure 7-2
- Without cooler, with insulation, see bottom right photo in Figure 7-2

The HFM 123732 (SB) was calibrated with 2 configurations:

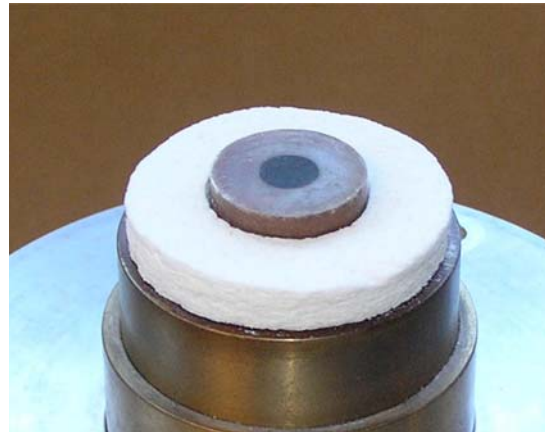
- Without cooler, with insulation
- Without cooler, without insulation

The HFM 701105 (SB) was calibrated with cooling system, without insulation.

The HFM 700263 (SB) was calibrated without cooling system, without insulation.



With cooler, without insulation



With cooler, with insulation



Without cooler, without insulation



Without cooler, with insulation

**Figure 7-2 The four mounting configurations used for HFM 123731 (G)**

When the heat flux meter is mounted flush with the wall, the radiation received by the sensor is easier to calculate than when the standard procedure is used. The heat flux is given by

$$q_{rad.received}'' = \sigma T_f^4 \quad (7-1)$$

The results of the calibrations are resumed in Table 7-1 - Table 7-4 below. The differences between the calibrations are calculated, using the first configuration as reference. The calibrations with the standard procedure and the calibrations from SINTEF-NBL are also compared.  $q$  is the total heat flux received by the sensor ( $\text{kW}/\text{m}^2$ ).

**Table 7-1 Results of comparisons for HFM 123731 (G)**

configuration	equation	q (kW/m <sup>2</sup> ) at 5 mV	difference
cooler, no insulation	$q=11.37u-0.3662$	56,48	
no cooler, no insulation	$q=11.329u-0.6606$	55,98	-0,89 %
cooler, insulation	$q=11.377-0.5616$	56,32	-0,28 %
no cooler, insulation	$q=11.332-0.5752$	56,08	-0,71 %
standard procedure	$q=11.723x+0.6442$	59,26	4,68 %
sintef	$q=11.302u+0.0459$	56,56	0,13 %

**Table 7-2 Results of comparisons for HFM 123732 (SB)**

configuration	equation	q (kW/m <sup>2</sup> ) at 5 mV	difference
no insulation	$q=11.924u-1.4994$	58,12	
insulation	$q=12.026u-1.778$	58,35	0,40 %
standard procedure	$q=12.442u-0.05$	62,16	6,50 %
Sintef	$q=12.004u-0.4449$	59,58	2,44 %

**Table 7-3 Results of comparisons for HFM 701105 (SB)**

configuration	equation	q (kW/m <sup>2</sup> ) at 5 mV	difference
cooler, no insulation	$q=4.7468u-0.6582$	23,08	
standard procedure	$q=4.9823u-0.1087$	24,80	6,96 %

**Table 7-4 Results of comparisons for HFM 700263 (SB)**

configuration	equation	q (kW/m <sup>2</sup> ) at 5 mV	difference
no cooler, no insulation	$q=1.8133u+0.1053$	9,17	
standard procedure	$q=1.9644u-0.0639$	9,76	6,01 %

According to the results of 123731 (G) calibrations, it can be concluded that the use of the cooler does not influence the results. Further, according to the results of 123731 (G) and 123732 (SB) calibrations, it can also be concluded that the use of the insulation does not influence the results.

The comparison between the calibration flush with the wall and the calibration with the insert shows a difference between 4.7% for the 123731 (G) gauge to 7% for the 701105 (SB) gauge. Indeed, for the calibration with standard procedure, the convection is reduced to a minimum, which is not the case when the sensor is flush in the wall. Therefore, in order to calculate the heat flux received by the sensor when it is flush in the wall, the heat transfer by convection has to be added. This explains the difference between the 2 calibrations.

## 8 Convective contribution in the SP furnace

The heat flux gauges are sensitive both to radiation and convection. Although the SP furnace is built to minimize the convection and therefore the convection is neglected in calibration calculations, it is important to estimate it in order to justify this assumption. Three different methods to estimate the convection in the furnace are presented.

### 8.1 Heat balance on the gauge

A schematic drawing of a heat flux sensor is shown in Figure 8-1.

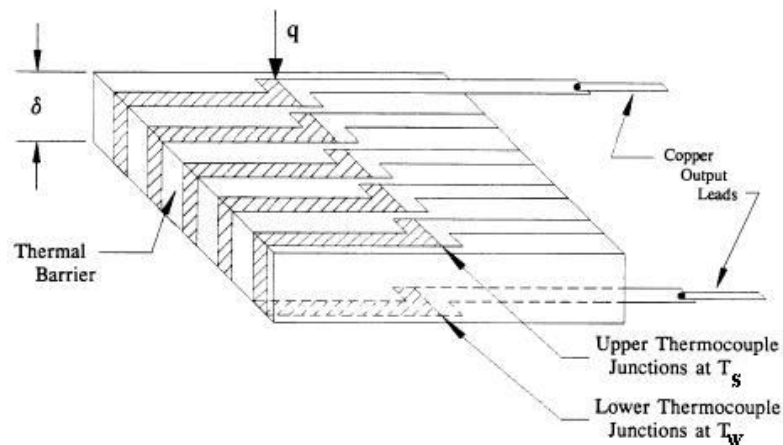


Figure 8-1 Thermopile heat flux sensor

Figure 8-2 displays the sensor surface of the Schmidt-Boelter heat flux gauge, which is subject to radiative heat transfer due to radiant source and convection due to a cross flow. It is assumed that no heat is transferred radially by conduction, but only axially, since the temperatures on the top surface and bottom surface are assumed to be uniform.

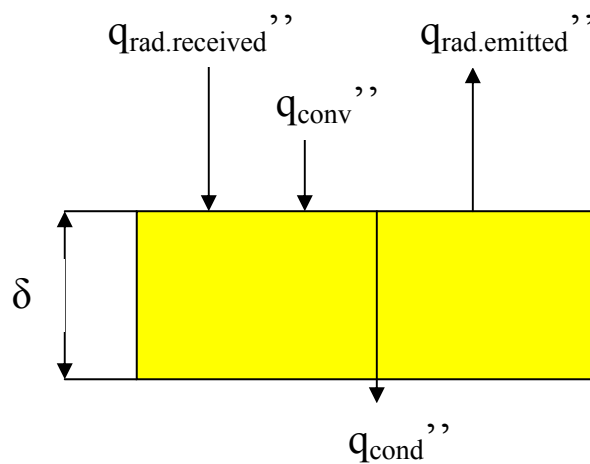


Figure 8-2 Energy balance at heat flux gauge surface

The heat flux energy balance can be written as:

$$q_{rad.received}'' - q_{rad.emitted}'' + q_{conv}'' = q_{cond}'' \quad (8-1)$$

Where:

$$\bullet \quad q_{rad.received}'' = \sigma \phi T_f^4 \quad (8-2)$$

$$\bullet \quad q_{rad.emitted}'' = \sigma T_s^4 \quad (8-3)$$

$$\bullet \quad q_{conv}'' = h(T_s - T_a) \quad (8-4)$$

$$\bullet \quad q_{cond}'' = \frac{k}{\delta}(T_s - T_w) \quad (8-5)$$

## 8.2 Determination of the convective part

The purpose is to evaluate the convective term,  $q_{conv}''$ , and compare this one with the radiative term,  $q_{rad}'' = q_{rad.received}'' - q_{rad.emitted}''$ .

$q_{rad.received}''$  is the radiation received by the sensor, i.e. the term calculated by the calculation procedure. To evaluate the radiative term, the radiation emitted by the sensor is needed, which means  $T_s$  is needed. It is worth noticing that the radiation received is much higher than the radiation emitted, so the value of  $T_s$  does not influence the result a lot.

If the conductive part is calculated, then it will be easy to obtain the convective part, just doing the difference between the  $q_{cond}$  and  $q_{rad}$ .

## 8.3 1<sup>st</sup> Method – Heat balance

To evaluate the convective part, the difference between  $T_s$  and  $T_w$  is needed. This difference of temperature is the difference of temperature between the upper and the lower junction of the thermopile. It seems to be difficult to measure these 2 temperatures 'manually'.

But it exists a correlation between this difference of temperature and the output voltage measured. Indeed

$$\Delta T = -0.6223\left(\frac{u}{N}\right)^2 + 25.826\frac{u}{N} + 0.0061 \quad (8-6)$$

This approximation is done using the table in Annex E.

Since the measure of the output voltage is known, the difference of temperatures  $\Delta T$  is deduced. This method seems to be good, since the measurement of the output voltage take account of both convective and radiative heat transfer.

Finally, the heat conducted through the material is known. The radiative part is given by the calculation that is done in connection to the calibration procedure. The difference gives the value of heat transfer by convection. The problem is that the conductivity  $k$ , the distance between the upper and the lower junction  $\delta$ , and the number of junctions  $N$  are not known so far. Some assumptions therefore have been done.

### 8.3.1 Assumptions

It is assumed that the thermopile is made of constantan, therefore  $k=23$  W/mK. The thickness of the thermopile is  $\delta=1.57$  mm, through measurements on the HFM 300073. This gauge was not used for the calculations, but only for the study of the structure of the gauge. The number of junction is assumed to be 25.

### 8.3.2 Results

The results are presented in Table 8-1. The data used come from the calibration of the heat flux meter 701105 (SB) performed the 15<sup>th</sup> of April 2005.

Table 8-1 Calculation of the heat transfer by convection

Tf (K)	Tw (K)	q (W/m <sup>2</sup> )	$\phi$	u (mV)	$\Delta T$
640.1	298.6	4588.1	0.482	0.93	1.0
761.5	298.3	9416.6	0.494	1.91	2.0
907.5	298.6	19230.5	0.500	3.89	4.0
1003.6	298.7	28872.8	0.502	5.83	6.0
1076.8	298.3	38355.9	0.503	7.73	7.9
1138.4	298.5	47967.1	0.504	9.63	9.9

Ts (K)	q <sub>cond</sub> (W/m <sup>2</sup> )	q <sub>rad</sub> (W/m <sup>2</sup> )	q <sub>conv</sub> (W/m <sup>2</sup> )	q <sub>conv</sub> /q <sub>rad</sub>
299.5	13951.5	4131.8	9819.7	2.4
300.3	28832.6	8955.7	19876.8	2.2
302.6	58591.2	18755.0	39836.2	2.1
304.7	87667.6	28384.2	59283.4	2.1
306.3	116007.7	37857.0	78150.7	2.1
308.3	144418.2	47454.5	96963.7	2.0

As seen in the table, the result implies that the convection is larger than the radiation which cannot be true.

### 8.3.3 Uncertainties in the model

It is assumed that  $k=23$  W/mK, but most of the times the manufacturer add some wafer on the thermopile, this can influence the value of  $k$ . The thickness is set to  $\delta=1.57$ mm, but this is the thickness of not only the thermopile but also possible protective material such as epoxy. In theory  $\delta$  is the distance between the lower and the upper junction. Moreover, it is assumed that the number of junctions is 25. If this figure is incorrect then it will result in an incorrect value of  $\Delta T$ . In order to reach reasonable values the number of junctions should be 75.

## 8.4 2<sup>nd</sup> Method - Calculation with femlab

Femlab is used to model the temperature distribution in the sensor in order to evaluate  $\Delta T$ . The heat flux meter is modelled as described Figure 8-3. Three parts of the heat flux meter are modelled: the sensor, the body, and the cooling system.

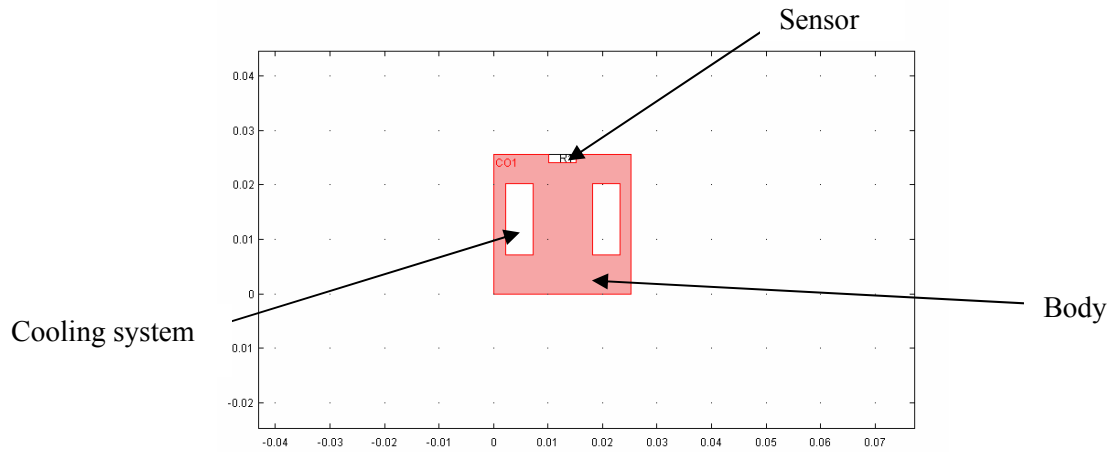


**Figure 8-3 Geometry modelling**

The dimensions used are the dimensions measured on the HFM 300073. This gauge was not used for the calibration work reported in chapters 6 and 7. It was an old gauge that had been taken out of use at SP and it was therefore allowed to be cut in halves to make it possible to study the build-up.

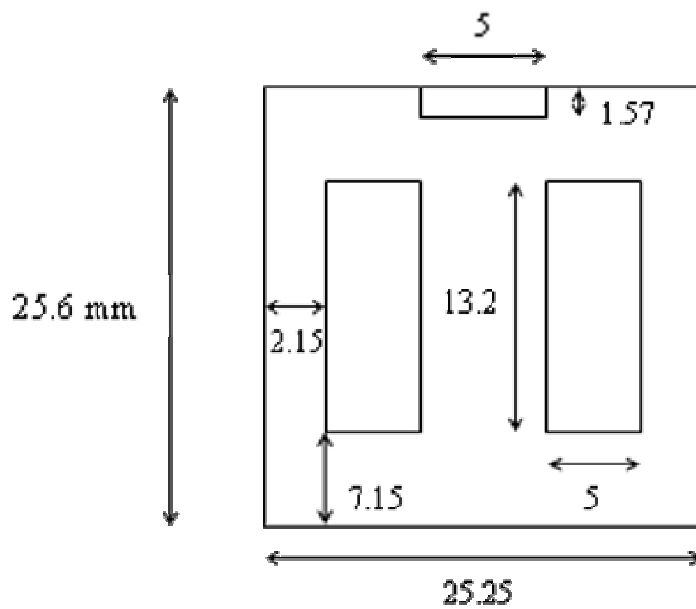


**Figure 8-4 Dimensions of the gauge**

As a boundary condition,  $T_w$  is applied on the surface in red on the figure below.

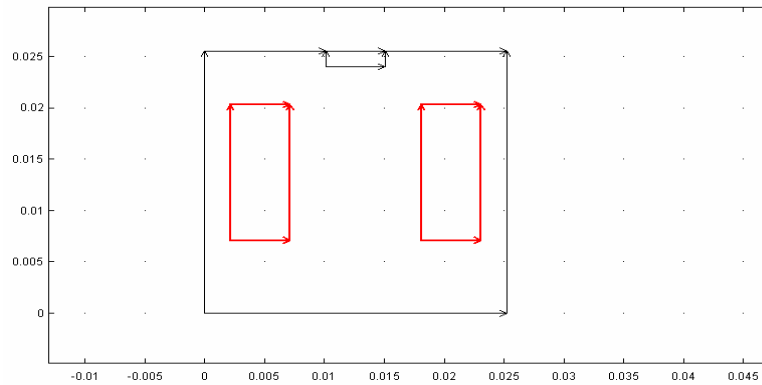


**Figure 8-5**  $T_w$  is applied on the surface in red

A heat flux is applied at the surface of the sensor.

$$\mathbf{n} \cdot (k \nabla T) = \varepsilon \sigma (T_{fe\text{mlab}}^4 - T^4) \quad (8.7)$$

The radiative temperature  $T_{fe\text{mlab}}$  is calculated from  $\phi T_f^4 = T_{fe\text{mlab}}^4$ . (8.8)

The sensor is assumed to be made of constantan, with  $k=23$  W/mK,  $\rho=8900$  kg/m<sup>3</sup> and  $C_p=400$  J/kgK. The body is assumed to be made of copper, with  $k= 400$  W/mK,  $\rho=8700$  kg/m<sup>3</sup>, and  $C_p= 385$  J/kgK.

An example of the distribution of temperature inside the gauge is shown on the figure below

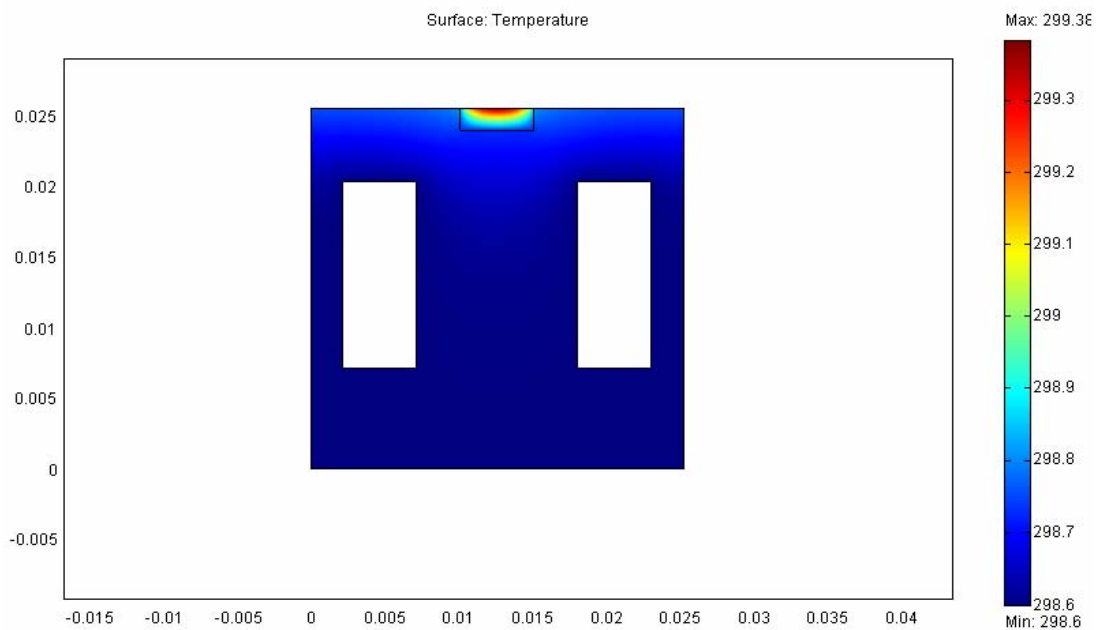


**Figure 8-6** Example of the distribution of temperature inside the gauge

Finally, for different values of heat flux applied on the surface of the sensor, and for different values of  $T_w$ , the values of temperatures on the top and the bottom of the sensor are deduced.

$T_{up}$  is the temperature on the top of the sensor, i.e. the temperature of the upper junction, and  $T_{low}$  is the temperature on the bottom of the sensor, i.e. the temperature of the lower junction.

The results are shown in Table 8-2. The data from the calibration of the HFM 701105 (SB) are used.

Assumptions:  $\delta=1.57\text{mm}$ ,  $k=23\text{ W/mK}$ .

**Table 8-2 Calculation of the heat transfer by convection**

Tf (K)	$T_{femlab}$ (K)	$T_w$ (K)	$q$ (W/m <sup>2</sup> )	$\phi$	u (mV)	$T_{up}$ (K)
640.1	533.4	298.6	4588.1	0.482	0.93	298.7
761.5	638.4	298.3	9416.6	0.494	1.91	298.9
907.5	763.1	298.6	19230.5	0.500	3.89	300.0
1003.6	844.7	298.7	28872.8	0.502	5.83	300.7
1076.8	906.9	298.3	38355.9	0.503	7.73	301.1
1138.4	959.0	298.5	47967.1	0.504	9.63	301.9

$T_{low}$ (K)	$q_{cond}$ (W/m <sup>2</sup> )	$q_{rad}$ (W/m <sup>2</sup> )	$q_{conv}$ (W/m <sup>2</sup> )	$q_{conv}/q_{rad}$
298.6	879.0	4136.9	-3257.9	-0.79
298.4	7998.7	8963.8	-965.0	-0.11
298.9	16451.6	18771.4	-2319.8	-0.12
299.1	24860.5	28409.0	-3548.5	-0.12
298.8	33269.4	37889.9	-4620.5	-0.12
299.1	41912.7	47495.9	-5583.1	-0.12

$q_{rad}$  is greater than  $q_{cond}$  and that implies negative values for  $q_{conv}$ . This comes from the fact that for the calculations, it is assumed that the temperature is uniform on the surface of the sensor, so the heat transfer by conduction on the side of the sensor is neglected. The value of  $q_{cond}$  calculated therefore is lower than the real value.

What is important to quote is that the value of  $q_{rad}$  and  $q_{cond}$  are of the same order, which implies low values for  $q_{conv}$ .

It is also worth noticing that the convective part is much greater for lower heat fluxes (lower values of temperature).

The problem of these calculations is that a very small difference in the input data influences the result significantly. For example, in Table 8-3 below, the heat transfer by conduction, radiation and convection are calculated again, but with a temperature of the upper junction increased by 0.3°C.

**Table 8-3 Calculation of convection with an increased value of  $T_{up}$** 

$T_{up}$ (K)	$T_{low}$ (K)	$q_{cond}$ (W/m <sup>2</sup> )	$q_{rad}$ (W/m <sup>2</sup> )	$q_{conv}$ (W/m <sup>2</sup> )	$q_{conv}/q_{rad}$
299.0	298.6	5273.9	4135.1	1138.8	0.28
299.2	298.4	12393.6	8961.9	3431.7	0.38
300.3	298.9	20846.5	18769.6	2076.9	0.11
301.0	299.1	29255.4	28407.1	848.3	0.03
301.4	298.8	37664.3	37888.1	-223.7	-0.01
302.2	299.1	46307.6	47494.0	-1186.4	-0.02

As can be seen, the results are different than those summarized in Table 8-2. This means that a very small difference in the input data influences the result. In the calculations of temperature with femlab, the convection is not taken in account. Therefore the temperatures calculated are probably wrong. Even if the convection is low, it is large enough to influence the result of the modelling.

The calculation of the convective part depends on the value of  $\Delta T$ , i.e. the temperature difference between the lower and the upper junction.

Comparing the two different methods to evaluate  $\Delta T$  shows that the 1<sup>st</sup> is the more accurate. Since the convection is neglected in the femlab simulation, the value of  $\Delta T$  given by this method is not fully correct and the results are very sensitive to small changes in the value of  $\Delta T$ . It is assumed that the first method gives accurate results, as the measurement of the output voltage is accurate. But for that calculation the problem is that the number of junctions  $N$ , the thermal conductivity of the thermopile, and its thickness are needed.

Then the conductive part can be easily evaluated using the relation

$$q_{cond} = \frac{k}{\delta} \Delta T \quad (8-9)$$

$$\text{With } \Delta T = -0.6223\left(\frac{u}{N}\right)^2 + 25.826\frac{u}{N} + 0.0061 \quad (8-10)$$

The radiative part is (as mentioned in 8.3) calculated in connection to the calibration procedure. And finally the convective part is deduced.

## 8.5 3<sup>rd</sup> Method– Direct method using the of air flow velocity

Another approach could be to investigate to evaluate the convective contribution in the SP furnace.

The airflow across the gauge is assumed to be laminar. This assumption is valid, since the Reynolds number at the gauge surface is much lower than the critical Reynolds number required for transition to turbulent flow.

At an air temperature of 50°C, the kinematic velocity  $\nu = 1.83e-5$  m<sup>2</sup>/s. The diameter of the sensor is approximately 5mm, and the velocity of the airflow should not be more than 0.1 m/s. So the maximum value of the Reynolds number is

$$R_e = \frac{V * d}{\nu} = 27.3 \quad (8-11)$$

This value is much lower than 6000, the approximate value of the critical Reynolds number.

Therefore, the following equation estimates the convective heat flux at the gauge surface [7].

$$q_{conv}'' = h(T_s - T_a) = \frac{0.664V^{1/2} Pr^{1/3} k_{air}}{\nu^{1/2} d^{1/2}} \quad (8-12)$$

The properties of air, thermal conductivity,  $k_{air}$ , kinematic viscosity,  $\nu$ , and Prandtl number, Pr (ratio of kinematic viscosity and thermal diffusivity) are calculated at the film temperature for the gauge surface  $T_{film} = \frac{T_s + T_a}{2}$ . (8-13)

$V$  ( $\text{ms}^{-1}$ ) is the velocity of the air flow, and  $d$  (m) is the diameter of the gauge.

### 8.5.1 Calculation of ambient temperature $T_a$

The ambient temperature ( $T_a$ ) close to the sensor is not known but as an approximation, it was assumed to be equal to T/C 7 in Olsson's report [6].

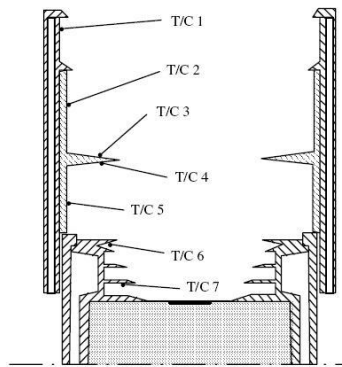


**Figure 8-7** Cross section of the cooler, with locations of the thermocouple (T/C 1 to 7) used in the experiments

Measures were taken for different fluxes and curves Figure 8-8 were plotted, the chart is from Olsson's report [6].

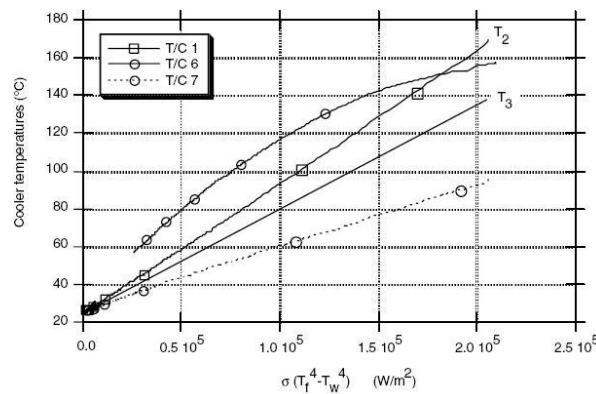


**Figure 8-8** The temperature of various part in the cooler without the fitting piece inserted

A linear regression was made on the curve for T/C 7 using several points read on the curve and the equation found was

$$T / C \cdot 7 = 3e - 4 * (\sigma(T_f^4 - T_w^4)) + 27.222 \quad (8-14)$$

Where  $T_f$  is the furnace temperature ( K )  
 $T_w$  is the water cooling temperature ( K )

The temperature  $T_a$  is given when the spacer ring is not inserted.

### 8.5.2 Measurement of ambient temperature $T_a$

Measures have been performed to confirm the results obtained by linear regression on Olsson's curves. The thermocouple used for these measurements was a very thin thermocouple, to avoid that the radiation received by the thermocouple influences the results.

The results are presented in Table 8-4, for different values of the furnace temperature  $T_f$  and are compared with the results from the linear regression.

**Table 8-4 Determination of temperature close to the sensor**

Tf (°C)	Tw (°C)	T <sub>measured</sub> (°C)	T <sub>calculated</sub> (°C)
391.9	25.7	30.8	30.4
491.5	25.7	34.1	32.9
591.5	25.5	38.6	36.6
690.9	25.6	44.9	41.8

The results obtained by measurements and calculations are similar. Therefore the values obtained by linear regression will be used in further work.

### 8.5.3 Calculation of the heat transfer coefficient h

In accordance with equation (8-13)  $T_{film}$  varies between 300 K and 350 K. Therefore, h is calculated for two different temperatures, 300 K and 350 K. The properties of air [8], at these temperatures are presented in Table 8-5.

**Table 8-5 Properties of air**

temp of air	k <sub>air</sub> (W/mK)	v (m <sup>2</sup> /s)	α (m <sup>2</sup> /s)
300K	0.03	1.57E-05	2.22E-05
350K	0.03	2.08E-05	2.98E-05

$k_{air}$  is the thermal conductivity of air,  $v$  the kinematic viscosity, and  $\alpha$  the thermal diffusivity.

The value of h is calculated for different values of the velocity V. The results are presented in the Table 8-6:

**Table 8-6** Calculation of the heat transfer coefficient

V (m/s)	at 300K	at 350K
	h (W/m <sup>2</sup> K)	h (W/m <sup>2</sup> K)
0.01	5.5	5.5
0.02	7.8	7.8
0.03	9.6	9.5
0.04	11.1	11.0
0.05	12.4	12.3
0.06	13.6	13.4
0.07	14.7	14.5
0.08	15.7	15.5
0.09	16.6	16.5
0.1	17.5	17.3
0.2	24.8	24.5

The values do roughly not depend on the temperature of the air.

The convection is calculated by equation 8-12 and the results, for different values of  $T_f$ , are presented in Table 8-7. The maximum value of  $h$ , i.e. 24.8 W/m<sup>2</sup>K, is used in order to maximize the results.  $T_s$  is set to be 25°C, in order to maximize the results too.

**Table 8-7** Calculation of the convective part

T <sub>f</sub> (°C)	T <sub>a</sub> (°C)	T <sub>a</sub> -T <sub>s</sub>	q <sub>conv, max</sub> (W/m <sup>2</sup> )	q <sub>rad</sub> (W/m <sup>2</sup> )	q <sub>conv</sub> /q <sub>rad</sub>
400	30.6	5.6	138	5369	0.026
500	33.2	8.2	202	9675	0.021
600	37.0	12.0	297	16020	0.019
700	42.3	17.3	430	24963	0.017
800	49.6	24.6	611	37132	0.016
900	59.3	34.3	850	53225	0.016
1000	71.8	46.8	1160	74003	0.016

Even if the value of  $q_{conv}$  is maximized, taking the minimum value of  $T_s$  and the maximum value of  $h$ , the convective heat transfer represents in the worst case, 2.5% of the total heat transfer.

It is a valid assumption to neglect the convective part in the calculation procedure provided that an error of 2.5% of the total heat flux is allowed. If a better precision is required then a more thorough calculation of the convection must be performed and included in the total uncertainty budget.

## 9 Investigation of possible non-linearities in the calibration

The output voltage is approximately proportional to the temperature difference across the gauge, which is approximately proportional to the heat flux. The calibration curves show that a correlation of linearity exists between the output voltage measured and the heat flux calculated. The investigation of the linearity was done to find out if the calibration procedure could be simplified.

### 9.1 Heat balance on the gauge

As shown before, the heat flux energy balance can be written as:

$$q_{rad.received}'' - q_{rad.emitted}'' + q_{conv}'' = q_{cond}'' \quad (9-1)$$

Where:

$$\bullet \quad q_{rad.received}'' = \sigma\phi T_f^4 \quad (9-2)$$

$$\bullet \quad q_{rad.emitted}'' = \sigma T_s^4 \quad (9-3)$$

$$\bullet \quad q_{conv}'' = h(T_a - T_s) \quad (9-4)$$

$$\bullet \quad q_{cond}'' = \frac{k}{\delta}(T_s - T_w) \quad (9-5)$$

So

$$q_{rad.received}'' = \varepsilon\sigma T_s^4 + \frac{k}{\delta}(T_s - T_w) + h(T_s - T_a) \quad (9-6)$$

The difference of temperature given by the thermocouple is

$$T_s - T_w = au^2 + bu + c \quad (9-7)$$

$q_{rad.received}''$  can be rewritten as

$$q_{rad.received}'' = \frac{k}{\delta}(T_s - T_w) + h(T_w + T_s - T_w - T_a) + \varepsilon\sigma(T_w + T_s - T_w)^4 \quad (9-8)$$

By putting equation (9-7) into equation (9-8) and neglecting all terms of order  $u^3$  and higher,  $q_{rad.received}''$  can be deduced to

$$\begin{aligned} q_{rad.received}'' &= \frac{k}{\delta}c + h(c + (T_w - T_a)) + \varepsilon\sigma(T_w + c)^4 \\ &+ u \left[ \frac{k}{\delta}b + hb + \varepsilon\sigma(4b(T_w + c)^3) \right] \\ &+ u^2 \left[ \frac{k}{\delta}a + ha + \varepsilon\sigma(6b^2(T_w + c)^2 + 4a(T_w + c)^3) \right] = \alpha u^2 + \beta u + \gamma \end{aligned} \quad (9-9)$$

The table in Annex F [9] is used to find a correlation between the temperature difference across the gauge and the voltage measured. The calculated values are given in Figure 9-1.

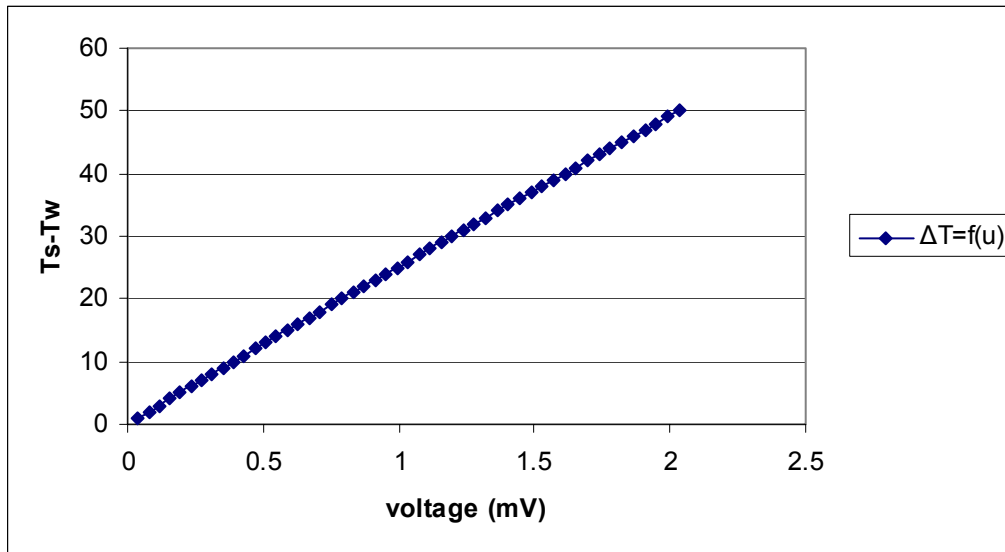


**Figure 9-1** The difference of temperature across the gauge as a function of the output voltage measured

The equation obtained (valid only in the range of temperature 0-50) is

$$T_s - T_w = -0.6223u^2 + 25.826u - 0.0061 \quad (9-10)$$

So  $a = -0.6223$

$b = 25.826$

$c = -0.0061$

Following values are used:

$k = 23 \text{ W/mK}$

$\delta = 1.57 \text{ mm}$

$T_w = T_a = 298 \text{ K}$

$h = 10 \text{ W/m}^2\text{K}$

The values of  $\alpha$ ,  $\beta$  and  $\gamma$  of the equation (9-8) are deduced

$\alpha = -9106.3$

$\beta = 378755.9$

$\gamma = 357.7$

so  $\alpha/\beta = 0.0009$

and  $\gamma/\beta = -0.024$

Therefore  $\alpha$  and  $\gamma$  could be neglected compared to  $\beta$  provided that errors up to 2 % are acceptable (the maximum value of  $u$  during the calibration is 25 mV). Thus it is a valid assumption to say

$$q_{rad.received}'' = \beta u \quad (9-11)$$

## 9.2 Simplification of the calibration

The number of points taken to calibrate a heat flux meter usually varies between 6 and 10 for a primary calibration. But the latency to have a temperature stable is long, therefore the time needed to perform a calibration is in the best case 15 hours. As can be seen in chapter 9.1 the theory permit to assume that the relation between the output voltage measured and the irradiance calculated is linear. Moreover, the calibration curves plotted are also linear. Therefore just one point would be enough to perform the calibration.

This part investigates the differences obtained in the calibration if the number of points used to the calibration is reduced to one.

The data from a six-point calibration of the heat flux meter 701105 (SB) have been used to evaluate what results a one-point calibration would give. The calibration curve obtained is shown in Figure 9-2.

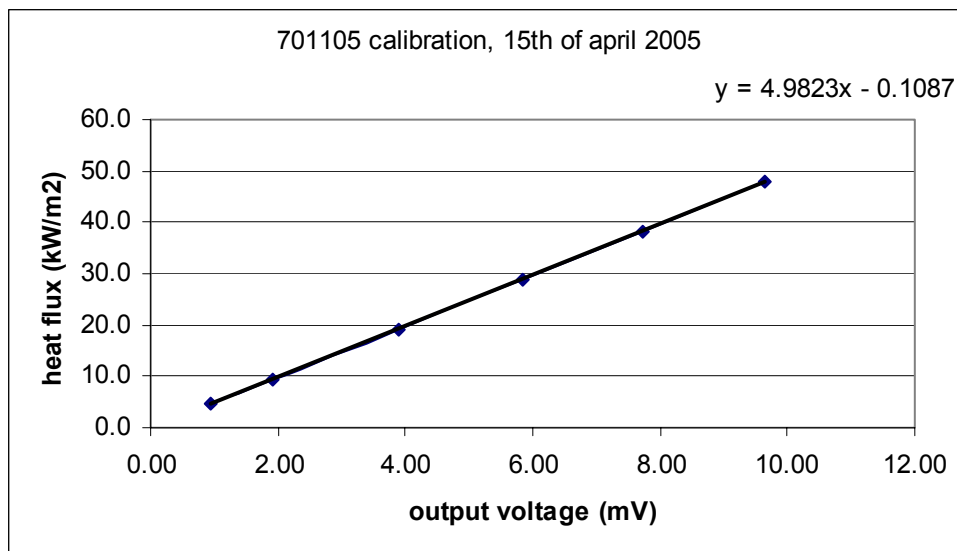


Figure 9-2 Calibration curve of the HFM 701105 (SB)

Table 9-1 displays the evaluation of a one-point calibration in comparison to the six-point calibration. A linear curve taking just two points: the point (0,0) and each of the 6 other points is plotted and equation are deduced. To be able to compare the results the heat flux is calculated a  $u=5$  mV, and the difference between this value, and the value obtained when all the points are used to draw the curve is calculated.

Table 9-1 Results of the '1-point' calibration

point	equation $q=au+b$		heat flux (kW/m <sup>2</sup> ) at $u=5mV$	difference
	a	b		
all points	4.9823	-0.1087	24.8	
linear regression	4.9666	0	24.8	0.12 %
1st point	4.9427	0	24.7	-0.36 %
2nd point	4.9202	0	24.6	-0.82 %
3rd point	4.9429	0	24.7	-0.36 %
4th point	4.9531	0	24.8	-0.15 %
5th point	4.9645	0	24.8	0.08 %
6th point	4.9787	0	24.9	0.36 %

As can be seen in the table, the difference is never more than 1%. This implies a good accuracy if the calibration is performed just with 1 point. The results for the other heat flux meters are given in Annex D. It is noticeable that for none heat flux meters calibrated, the difference was above 1%. Therefore, taking only one measurement to plot the calibration curve adds only about 1% error to the total uncertainty.

## 10 Conclusion

The new furnace has been thoroughly tested. Several calibrations were performed on seven different heat flux meters. The results obtained are quite similar from those obtained with the former one. The average difference is about 1% in term of heat flux. On further work, it could be possible to use a temperature corrected of about 0.3-0.4 % to decrease this difference.

The heat balance done on the Schmidt-Boelter gauge shows that the calibration can be considered linear. This assumption was confirmed by the calibrations performed in the project.

It appears difficult to calculate with accuracy the part of heat transferred by convection with the current data we have. Nevertheless the assumptions made to evaluate the convection have been maximized and the values of convection obtained are never more than 2.5% of the total heat flux.

## 11 References

- [1] *International Technical Specification - Fire tests-calibration and use of heat flux meters- Part 1: General principles*, ISO TS 14934-1:2002 (E). International Organization for Standardization, Geneva 2002.
- [2] *International Standard under development - Fire tests-calibration and use of heat flux meters- Part 2: Primary calibration methods*, ISO/FDIS 14934-2, to be FDIS balloted during 2005
- [3] *International Standard under development - Fire tests-calibration and use of heat flux meters- Part 3: Secondary calibration methods*, to be FDIS balloted
- [4] *International Standard under development - Fire tests-calibration and use of heat flux meters-Part 4: Guidance on the use of heat flux meters in fire tests*, to be published as Technical Specification
- [5] W. M. Pitts, A. V. Murthy, J. L. de Ris, J. R. Filtz, K. Nygård, D. Smith, I. Wetterlund, *Round Robin Study of Total Heat Flux Gauge Calibration at Fire Laboratories*, National Institute of Standards and Technology Special Publication 1031, Gaithersburg, MD, USA, 2004.
- [6] S. Olsson, *Calibration of Radiant Heat Flux Meters – The Development of a Water Cooled Aperture for Use with Black Body Cavities*, SP REPORT 1991:58, Borås, 1991.
- [7] R. A. Bryant, E. L. Johnsson, T. J. Ohlemiller, C. A. Womeldorf, *Estimates of the uncertainty of radiative heat flux calculated from total heat flux measurements-* National Institute of Standards and Technology Special Publication 971, Gaithersburg, MD, USA, 2001.
- [8] J.P. Holman, *Heat transfer* (seventh edition). McGraw-Hill Book Co, 1992 (ISBN 0-07-112644-9)
- [9] <http://www.thermometricscorp.com/thertypt.html>
- [9] <http://www.me.utexas.edu/~howell/tablecon.html>, *A catalog of radiation heat transfer configuration factors*, John R. Howell, University of Texas at Austin.

## Annex A Theory of the calculation

This theory was developed by Sören Olsson [6].

The aim of whatever calibration method used, is to be able to find a relationship between the irradiation (net radiative heat flux) to the gauge and the output voltage measured by the HFM. The net radiative heat flux is calculated according to a calculation procedure which implies the knowledge of water temperature and furnace temperature. The calibration is normally performed at several levels of heat flux. By using the deduced heat flux and the measured output voltage a relationship curve can be drawn.

### Radiating environment inside the cooler

The first step is to find an expression for the radiative heat flux. In order to form this expression, the radiating environment is divided into five separate parts, each radiating with different temperatures and emissivities. The parts are depicted in Figure A-1 showing a cross-section of the cooler with the spacer ring inserted. Both the case with the spacer ring and without it will be considered. Note that items with the exponent ' denotes entities with the spacer ring removed, while the exponent '' denotes entities with it inserted.

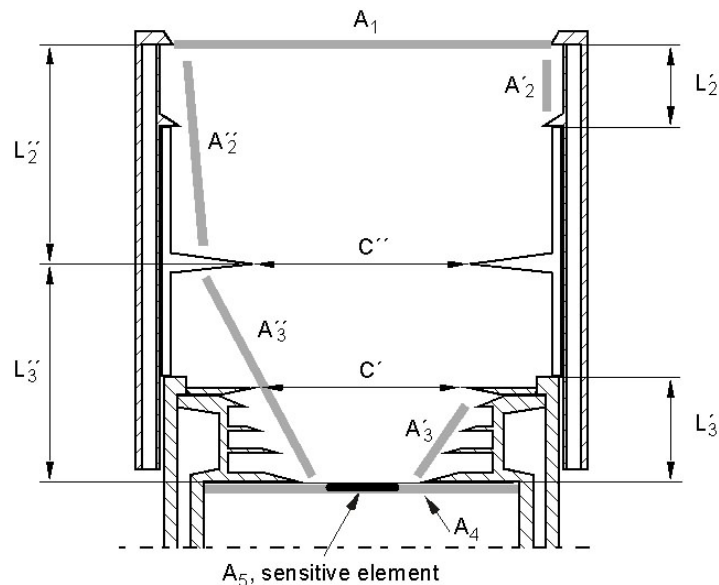


**Figure A-1** Cross-section of the cooler with movable insert and spacer ring in place. The grey-shaded lines indicate the different areas considered in the simplified calculation model. (With respect to the construction of the cooling system of the fixed cooler this figure reflects the old furnace. All flanges are equally designed in both furnaces)

The area  $A_1$  consists of the image of the furnace, which is radiating to the gage through the top aperture, with the temperature  $T_1$  and an apparent emissivity  $\varepsilon_1$ . Below that is the area  $A_2$ , i.e. the cylindrical surface with the height  $L'_2$  or  $L''_2$ , emissivity  $\varepsilon_2$  and temperature  $T'_2$  or  $T''_2$ , depending on the case. Note that the upper surface of the flange on the fitting piece is also included in  $A''_2$ . The areas  $A'_3$  and  $A''_3$ , representing the lowest section of the cooler, is restricted by the aperture  $C'$  or  $C''$ , with corresponding height  $L'_3$  or  $L''_3$ , emissivity  $\varepsilon_3$  and temperature  $T'_3$  or  $T''_3$ , respectively.

The bottom surface consists partly of the gage's sensing element area,  $A_5$ , with the unknown emissivity  $\varepsilon_5$  and temperature  $T_5$ . The fact that  $\varepsilon_5$  is not known, is not a problem, as it can be considered as a part of the gage's response function and set to unity. The temperature  $T_5$  may be considered the same as the cooling water temperature. The discrepancy from that may also be considered as a part of the response function.

The rest of the bottom surface (the ring surrounding  $A_5$ ), is considered as one entity, the area  $A_4$ . The emissivities and temperatures for that area are not entirely known, but the effect of it on the total energy balance is very small, and could also be considered as part of the gage response function. On the second hand,  $A_4$  consist of the rest of the cooler bottom, with a temperature very close to the cooling water temperature and an emissivity almost the same as for  $A_2$  and  $A_3$ . As the effects of these areas are small, it is justified to lump them together in one area,  $A_4$ , with emissivity  $\varepsilon_4$  and temperature  $T_4$ .

### Calculation of the net radiation heat flux with a simplified configuration

The calculation of the net heat flux to the gage can be made by using the *net-radiation method*. For the five areas given in Figure A-1, the following system of equations can be formed

$$\frac{q_i}{\varepsilon_i} - \sum_{k=1}^5 \frac{1 - \varepsilon_k}{\varepsilon_k} F_{ik} q_k = \sum_{k=1}^5 F_{ik} (e_{bi} - e_{bk}) \quad (\text{A.1})$$

where  $q_i$  = the net radiation per unit area leaving the area  $i$   
 $F_{ik}$  = the configuration factor for radiation leaving area  $i$  and reaching area  $k$   
 $\varepsilon_k$  = the emissivity for area  $k$   
 $e_{bi}$  = the blackbody radiation ( $\sigma T^4$ ) leaving area  $i$

#### Demonstration:

We can consider the furnace, the cooler with movable insert, and the heat flux meter as an enclosure composed of 5 discrete surface areas. The objectives are to analyze the radiation exchange between the surface areas. A complex radiative exchange occurs inside the enclosure as radiation leaves a surface, travels to other surfaces and is partially reflected. It would be complicated to follow the beams of radiation. But it's not necessary, we can use an analysis called *net-radiation method*.

We call  $q_i$  and  $q_o$  the rates of incoming and outgoing radiant energy per unit inside area. If  $A_k$  is the  $k$ th inside surface area of the enclosure,  $Q_k$  could be the heat conducted through the wall to  $A_k$ . Then

$$Q_k = q_k A_k = (q_{o,k} - q_{i,k}) A_k \quad (\text{A-2})$$

A second equation results from the fact that the energy flux leaving the surface is composed of emitted plus reflected energy. This gives

$$q_{o,k} = \varepsilon_k \sigma T_k^4 + (1 - \varepsilon_k) q_{i,k} \quad (\text{A-3})$$

The incident flux  $q_{i,k}$  is derived from the portions of the energy leaving the surfaces in the enclosure that arrive at the  $k^{\text{th}}$  surface. This gives

$$q_{i,k} = \sum_{j=1}^N F_{kj} q_{o,j} \quad (\text{A-4})$$

Equations (2) and (3) provide two different expressions for  $q_{i,k}$ . If we substitute each in eq. (2) to eliminate  $q_{i,k}$  we obtain

$$q_k = \frac{\varepsilon_k}{1 - \varepsilon_k} (\sigma T_k^4 - q_{o,k}) \quad (\text{A-5})$$

$$q_k = q_{o,k} - \sum_{j=1}^N F_{kj} q_{o,j} = \sum_{j=1}^N F_{kj} (q_{o,k} - q_{o,j}) \quad (\text{A-6})$$

Now write these two equations for each of the five surfaces:

$$q_1 = \frac{\varepsilon_1}{1 - \varepsilon_1} (\sigma T_1^4 - q_{o,1})$$

$$q_1 = q_{o,1} - F_{11} q_{o,1} - F_{12} q_{o,2} - F_{13} q_{o,3} - F_{14} q_{o,4} - F_{15} q_{o,5}$$

.....

$$q_5 = \frac{\varepsilon_5}{1 - \varepsilon_5} (\sigma T_5^4 - q_{o,5})$$

$$q_5 = q_{o,5} - F_{51} q_{o,1} - F_{52} q_{o,2} - F_{53} q_{o,3} - F_{54} q_{o,4} - F_{55} q_{o,5}$$

The first of each of these 5 pairs of equation is solved for  $q_{o,i}$  ( $i=1 \dots 5$ ).

The  $q_{o,i}$  are substituted into the second equation of each pair to obtain:

$$q_1 \left( \frac{1}{\varepsilon_1} - F_{11} \frac{1 - \varepsilon_1}{\varepsilon_1} \right) - q_2 F_{12} \frac{1 - \varepsilon_2}{\varepsilon_2} - q_3 F_{13} \frac{1 - \varepsilon_3}{\varepsilon_3} - q_4 F_{14} \frac{1 - \varepsilon_4}{\varepsilon_4} - q_5 F_{15} \frac{1 - \varepsilon_5}{\varepsilon_5}$$

$$= (1 - F_{11}) \sigma T_1^4 - F_{12} \sigma T_2^4 - F_{13} \sigma T_3^4 - F_{14} \sigma T_4^4 - F_{15} \sigma T_5^4$$

.....

$$- q_1 F_{51} \frac{1 - \varepsilon_1}{\varepsilon_1} - q_2 F_{52} \frac{1 - \varepsilon_2}{\varepsilon_2} - q_3 F_{53} \frac{1 - \varepsilon_3}{\varepsilon_3} - q_4 F_{54} \frac{1 - \varepsilon_4}{\varepsilon_4} + q_5 \left( \frac{1}{\varepsilon_5} - F_{55} \frac{1 - \varepsilon_5}{\varepsilon_5} \right)$$

$$= -F_{51} \sigma T_1^4 - F_{52} \sigma T_2^4 - F_{53} \sigma T_3^4 - F_{54} \sigma T_4^4 + (1 - F_{55}) \sigma T_5^4$$

Using summation notation to write this for the  $k^{\text{th}}$  surface, eq (A-7) is derived

$$\sum_{j=1}^N \left( \frac{\delta_{kj}}{\varepsilon_j} - F_{kj} \frac{1 - \varepsilon_j}{\varepsilon_j} \right) q_j = \sum_{j=1}^N (\delta_{kj} - F_{kj}) \sigma T_j^4 = \sum_{j=1}^N F_{kj} \sigma (T_k^4 - T_j^4) \quad (\text{A-7})$$

Where, corresponding to each surface,  $k$  takes on one of the values  $1, 2, \dots, N$ , and  $\delta_{kj}$  is the Kronecker delta defined as

$$\delta_{kj} = \begin{cases} 1 & \text{when } k = j \\ 0 & \text{when } k \neq j \end{cases}$$

Finally, we obtain the result that we expected

$$\frac{q_i}{\varepsilon_i} - \sum_{k=1}^5 \frac{1 - \varepsilon_k}{\varepsilon_k} F_{ik} q_k = \sum_{k=1}^5 F_{ik} (e_{bi} - e_{bk}) \quad (\text{A-1})$$

Where  $q_i$  = the net radiation per unit area leaving the area  $i$   
 $F_{ik}$  = the configuration factor for radiation leaving area  $i$  and reaching area  $k$   
 $\varepsilon_k$  = the emissivity for area  $k$   
 $e_{bi}$  = the blackbody radiation ( $\sigma T^4$ ) leaving area  $i$

This equation system can then be solved for  $q_5$ , which is the radiation leaving the gage's sensitive element per unit area. As its emissivity is set to unity,  $-q_5$  is the irradiation, i.e. the entity which is looked for. The configuration factors, or view factors, represent the amount of energy which leaves one surface and reaches the other. For instance,  $F_{12}$  is the fraction of energy leaving surface 1 which reaches surface 2. The calculation of these factors is, in this case, difficult because of the geometry. That's why, to simplify the calculation, a cylindrical model of the enclosure is used, as shown in Figure A-2.

The notation in Figure A-2 is the same as in Figure A-1, with the exception that  $L_2$  and  $L_3$  shall be replaced with their corresponding measures  $L'_2$  or  $L''_2$ , and so on. Note also that the radius  $r_4$  for the whole bottom area is the same as  $r_1$ , the radius of the upper aperture.

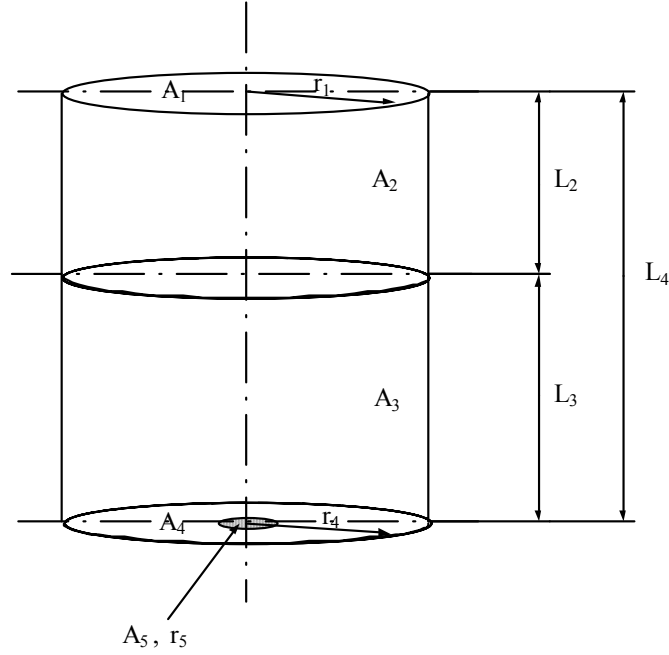


**Figure A-2 The cylindrical model of the enclosure, with the furnace aperture at the top and the gage at the bottom.**

In order to calculate  $q_5$ , several assumptions could be done. First of all, it's obvious that the view factors  $F_{11}$ ,  $F_{44}$ ,  $F_{45}$ ,  $F_{55}$ ,  $F_{54}$  are zero, as they are between flat surfaces in the same plane. Moreover, the radiation exchange between  $A_2$  and  $A_5$  is prevented due to the cooler's geometric shape thus  $F_{25} = F_{52} = 0$ .

And with the condition  $\varepsilon_5 = 1$ , Eq (A-1) can be rewritten as

$$\frac{q_1}{\varepsilon_1} - \frac{1-\varepsilon_2}{\varepsilon_2} F_{12} q_2 - \frac{1-\varepsilon_3}{\varepsilon_3} F_{13} q_3 - \frac{1-\varepsilon_4}{\varepsilon_4} F_{14} q_4 = \sum_1^5 F_{1k} (e_{b1} - e_{bk}) \quad (\text{A-8})$$

$$-\frac{1-\varepsilon_1}{\varepsilon_1} F_{21} q_1 + \frac{1-(1-\varepsilon_2)}{\varepsilon_2} F_{22} q_2 - \frac{1-\varepsilon_3}{\varepsilon_3} F_{23} q_3 - \frac{1-\varepsilon_4}{\varepsilon_4} F_{24} q_4 = \sum_1^5 F_{2k} (e_{b2} - e_{bk}) \quad (\text{A-9})$$

$$-\frac{1-\varepsilon_1}{\varepsilon_1} F_{31} q_1 - \frac{(1-\varepsilon_2)}{\varepsilon_2} F_{32} q_2 + \frac{1-(1-\varepsilon_3)}{\varepsilon_3} F_{33} q_3 - \frac{1-\varepsilon_4}{\varepsilon_4} F_{34} q_4 = \sum_1^5 F_{3k} (e_{b3} - e_{bk}) \quad (\text{A-10})$$

$$-\frac{1-\varepsilon_1}{\varepsilon_1} F_{41} q_1 - \frac{1-\varepsilon_2}{\varepsilon_2} F_{42} q_2 - \frac{1-\varepsilon_3}{\varepsilon_3} F_{43} q_3 + \frac{q_4}{\varepsilon_4} = \sum_1^5 F_{4k} (e_{b4} - e_{bk}) \quad (\text{A-11})$$

$$-\frac{1-\varepsilon_1}{\varepsilon_1} F_{51} q_1 - \frac{1-\varepsilon_2}{\varepsilon_2} F_{52} q_2 - \frac{1-\varepsilon_3}{\varepsilon_3} F_{53} q_3 + \frac{q_5}{\varepsilon_5} = \sum_1^5 F_{5k} (e_{b5} - e_{bk}) \quad (\text{A-12})$$

The four first equations are independent of  $q_5$ . So they can be solved as a separate system. The values of  $q_1$ ,  $q_2$ ,  $q_3$  and  $q_4$  are thus determined. And finally,  $q_5$  can be found by inserting these values in equation (10) and neglecting the second term on the left hand side since the cooler is designed to prevent reflections from  $A_1$  on  $A_3$  to  $A_5$ .

Note, however, that  $F_{53}$  and  $F_{35}$  can not be set to zero in the right hand side of the four first equations. Further on, correction has to be made for the fact that the geometry is not equal in the model and the reality. Setting the view factors  $F_{25}$ ,  $F_{52}$ ,  $F_{53}$  and  $F_{35}$  to zero, will introduce an error in the total radiation balance, due to the approximations in

the model. They have to be compensated for as they will affect the radiation exchange between the other parts of the enclosure. This is made by adding  $F_{25}$  to  $F_{22}$  and by expressing  $F_{53}$  as  $1-F_{51}$  in order to assure that the total sum of view factors is unity.

The calculation procedure is implemented as an Excel macro. The solving of the equation system is done by matrix algebra and is described in details below.

## Solving of equation matrix

The first step is to calculate  $q_1, q_2, q_3$  and  $q_4$ .

A matrix is used to express the equation system given in the previous part.

$$\begin{bmatrix} \frac{1}{\varepsilon_1} & -\frac{1-\varepsilon_2}{\varepsilon_2}F_{12} & -\frac{1-\varepsilon_3}{\varepsilon_3}F_{13} & -\frac{1-\varepsilon_4}{\varepsilon_4}F_{14} \\ -\frac{1-\varepsilon_1}{\varepsilon_1}F_{21} & \frac{1-(1-\varepsilon_2)F_{22}}{\varepsilon_2} & -\frac{1-\varepsilon_3}{\varepsilon_3}F_{23} & -\frac{1-\varepsilon_4}{\varepsilon_4}F_{24} \\ -\frac{1-\varepsilon_1}{\varepsilon_1}F_{31} & -\frac{1-\varepsilon_2}{\varepsilon_2}F_{32} & \frac{1-(1-\varepsilon_3)F_{33}}{\varepsilon_3} & -\frac{1-\varepsilon_4}{\varepsilon_4}F_{34} \\ -\frac{1-\varepsilon_1}{\varepsilon_1}F_{41} & -\frac{1-\varepsilon_2}{\varepsilon_2}F_{42} & -\frac{1-\varepsilon_3}{\varepsilon_3}F_{43} & \frac{1}{\varepsilon_4} \end{bmatrix} \begin{bmatrix} q_1 \\ q_2 \\ q_3 \\ q_4 \end{bmatrix} = \begin{bmatrix} \sum_{k=1}^5 F_{1k}(e_{b1} - e_{bk}) \\ \sum_{k=1}^5 F_{2k}(e_{b2} - e_{bk}) \\ \sum_{k=1}^5 F_{3k}(e_{b3} - e_{bk}) \\ \sum_{k=1}^5 F_{4k}(e_{b4} - e_{bk}) \end{bmatrix}$$

This is a matrix of the form

$$A * X = D \quad (\text{A-13})$$

The value of X is thus

$$X = INV(A) * D \quad (\text{A-14})$$

The values of  $q_1, q_2, q_3$  and  $q_4$  are so determined.

From the following equation

$$-\frac{1-\varepsilon_1}{\varepsilon_1}F_{51}q_1 - \frac{1-\varepsilon_2}{\varepsilon_2}F_{52}q_2 - \frac{1-\varepsilon_3}{\varepsilon_3}F_{53}q_3 + q_5 = \sum_{k=1}^5 F_{5k}(e_{b5} - e_{bk}) \quad (\text{A-15})$$

$q_5$  is therefore easily determined.

Note that the irradiation is  $-q_5$ .

## Calculation of view factors

This part shows how some view factors are calculated. However, the calculations done to find the equations are not described.

- The view factor from a disk in cylinder base (or top) to inside surface of right circular cylinder as shown in Figure A-3 is given by

$$F_{1-2} = \frac{1}{2} \left( 1 - R^2 - H^2 + \left[ (1 + R^2 + H^2)^2 - 4R^2 \right]^{1/2} \right) \quad (\text{A-16})$$

With  $R = r_2/r_1$  and  $H = h/r_1$

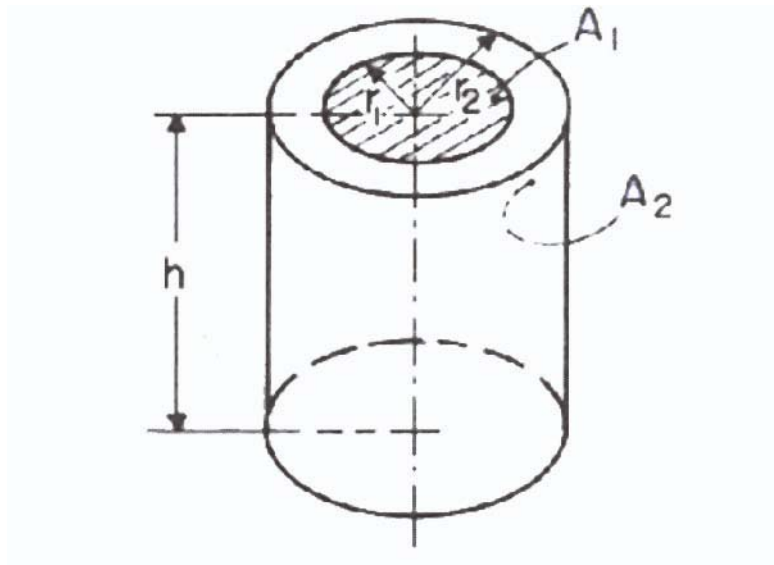


**Figure A-3** View factor from a disk in cylinder base to inside surface of right circular cylinder

With this equation  $F_{12}$ ,  $F_{13}$ ,  $F_{52}$ ,  $F_{53}$  are easily calculated.

- The view factor from an annular ring on cylinder base (or top) to inside surface of right circular cylinder as shown in Figure A-4 is given by

$$F_{1-2} = \frac{1}{2} \left( 1 + \frac{1}{(R^2 - 1)} \left\{ H(4R^2 + H^2)^{1/2} - \left[ (1 + R^2 + H^2)^2 - 4R^2 \right]^{1/2} \right\} \right) \quad (\text{A-17})$$

With  $R = r_2/r_1$  and  $H = h/r_1$

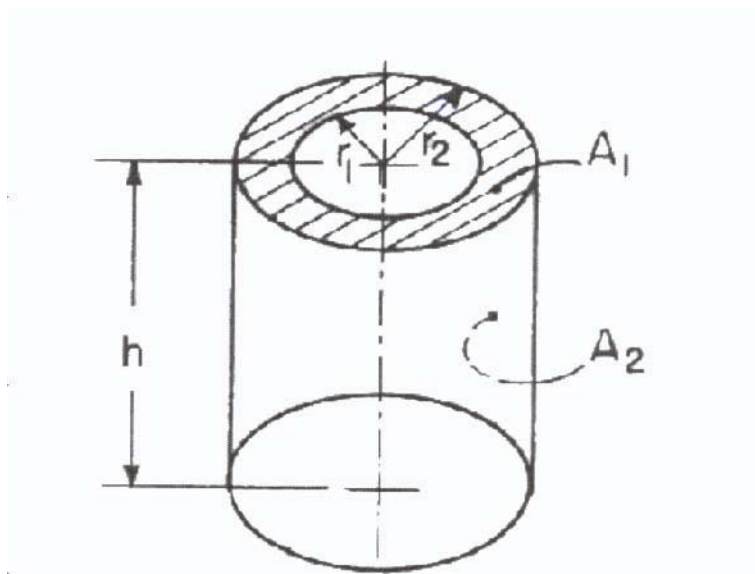


**Figure A-4** View factor from an annular ring on cylinder base to inside surface of right circular cylinder

With this equation  $F_{42}$ ,  $F_{43}$  are easily calculated.

- The view factor from a disk to a parallel coaxial disk as shown in Figure A-5 is given by

$$F_{1-2} = \frac{1}{2} \left\{ X - \left[ X^2 - 4 \left( \frac{R_2}{R_1} \right)^2 \right]^{\frac{1}{2}} \right\} \quad (\text{A-18})$$

With  $R = r/a$  and  $X = 1 + \frac{(1 + R_2^2)}{R_1^2}$

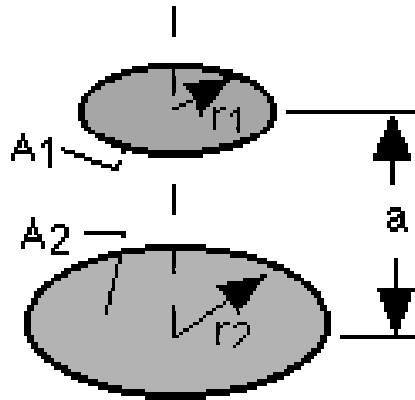


Figure A-5 View factor from a disk to a parallel coaxial disk

With this equation,  $F_{15}$  is easily calculated.

- The view factor from a disk to coaxial annular ring on parallel disk as shown in Figure A-6 is given by

$$F_{1-2} = \frac{1}{2} \left\{ R_3^2 - R_2^2 - \left[ (1 + R_3^2 + H^2)^2 - 4R_3^2 \right]^{\frac{1}{2}} + \left[ (1 + R_2^2 + H^2)^2 - 4R_2^2 \right]^{\frac{1}{2}} \right\} \quad (\text{A-19})$$

With  $H = a/r_1$  ;  $R_2 = r_2/r_1$  ;  $R_3 = r_3/r_1$

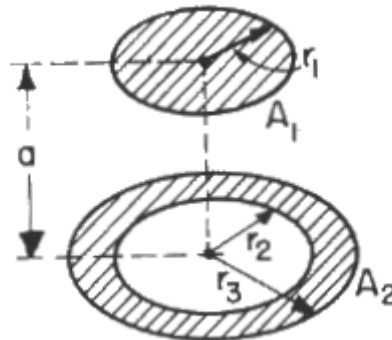


Figure A-6 View factor from a disk to coaxial annular ring on parallel disk

With this equation, we can easily calculate  $F_{14}$ .

- To calculate some view factors, some relations are useful.

A very useful relation is called the ‘reciprocity relation’.

It applies in a general way for any two surfaces  $m$  and  $n$ :

$$A_m F_{mn} = A_n F_{nm} \quad (\text{A-20})$$

Moreover, in an enclosure, the sum of view factors is equal to 1.

For instance, in our case, we can write that

$$F_{12} + F_{13} + F_{14} + F_{15} = 1 \quad (\text{A-21})$$

In order to simplify the calculation of some view factors, we introduce two areas,  $A_6$  and  $A_7$ , which are only construction areas.

$A_6$  is the area of the disk between  $A_2$  and  $A_3$ .

$A_7$  is the area corresponding to the sum of  $A_4$  and  $A_5$ .

These areas are useful to calculate some view factors.

For example

$$F_{34} = F_{37} - F_{35}$$

$$F_{23} = 1 - F_{21} - F_{22} - F_{27}$$

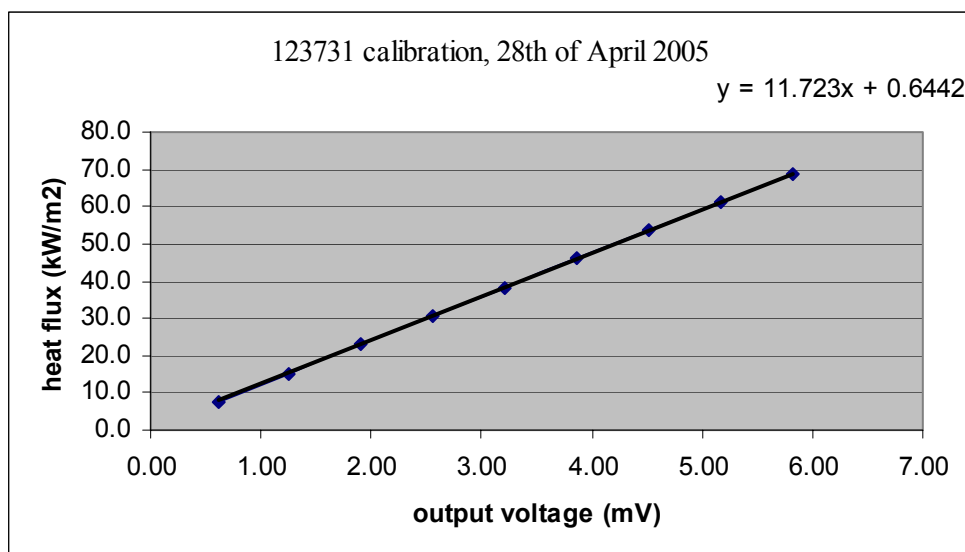
## Annex B Results of the calibrations using standard procedure

All calibrations performed before the 5<sup>th</sup> of May were performed with Imp5. Calibrations after that date were performed with an uncalibrated Imp borrowed from Solartron. A comparison performed with gauge 123731 (G) showed very similar results and therefore the borrowed Imp was not calibrated.

### HFM 123731 (G)

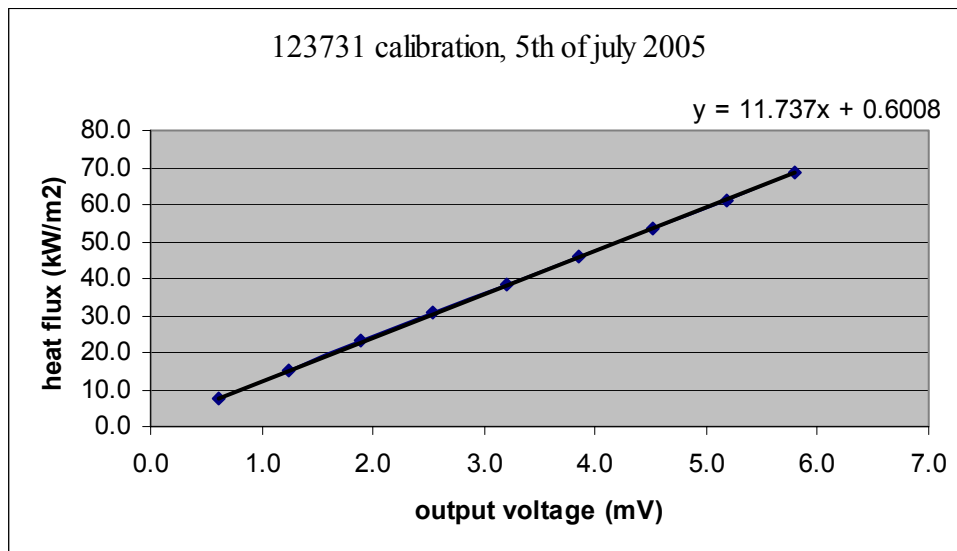
- Calibration performed the 28<sup>th</sup> of April 2005 (with Imp 5).

Tw (°C)	Tf (°C)	output voltage (mV)	heat flux (kW/m <sup>2</sup> )
25.8	447.4	0.61	7.5
25.3	584.5	1.25	15.3
25.5	676.9	1.90	23.1
25.5	746.2	2.55	30.7
25.4	804.0	3.20	38.4
25.3	853.3	3.86	45.9
25.4	897.4	4.52	53.6
25.4	936.1	5.16	61.1
25.6	971.7	5.82	68.7



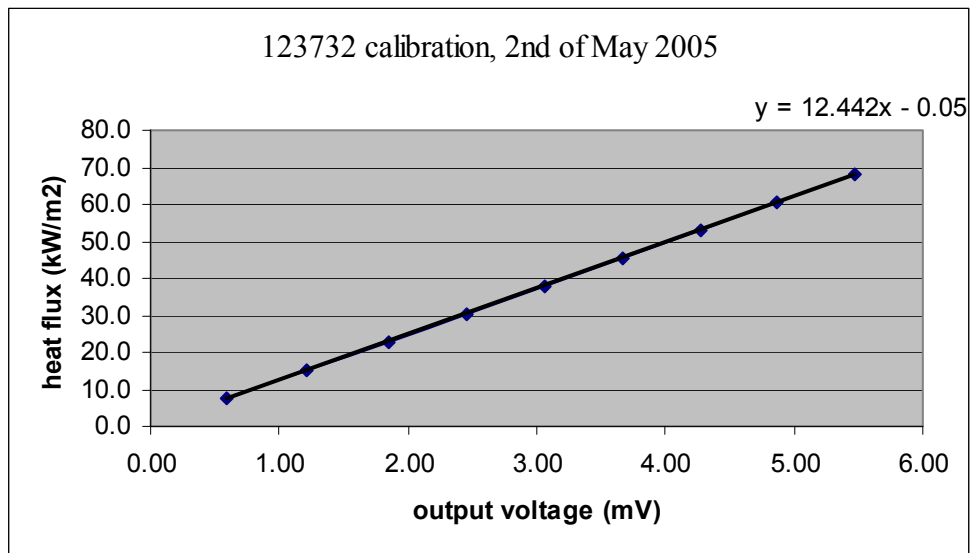
- Calibration performed the 5<sup>th</sup> of July 2005 (with Imp 49).

Tw (°C)	Tf (°C)	ouput voltage (mV)	heat flux (kW/m2)
26.1	447.0	0.6	7.5
26.1	584.0	1.3	15.2
26.1	676.3	1.9	23.0
26.1	745.6	2.5	30.6
25.8	803.4	3.2	38.2
25.4	853.4	3.8	45.9
25.8	897.5	4.5	53.6
26.1	936.3	5.2	61.1
26.0	971.6	5.8	68.6



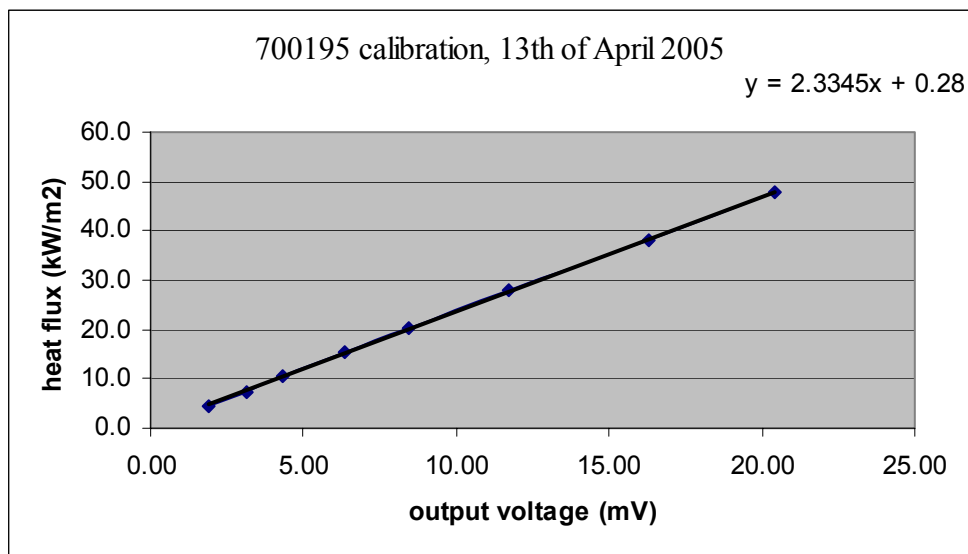
**HFM 123732 (SB)**

Tw (°C)	Tf (°C)	ouput voltage (mV)	heat flux (kW/m2)
25.5	447.5	0.60	7.4
24.3	584.5	1.22	15.1
25.0	677.0	1.85	22.9
25.7	746.1	2.45	30.4
25.6	803.8	3.06	38.0
24.8	853.4	3.67	45.6
25.4	897.4	4.28	53.1
25.9	935.8	4.86	60.5
25.9	971.3	5.47	68.0



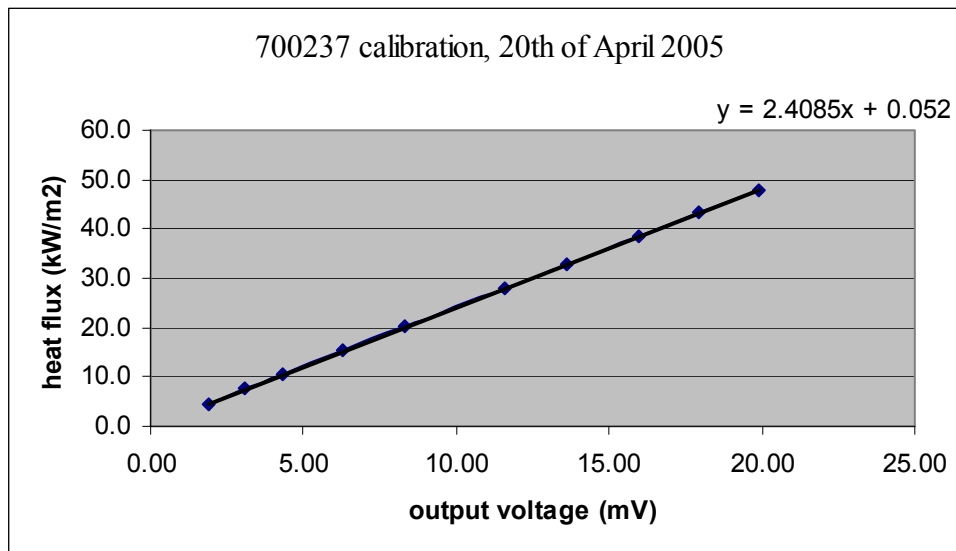
**HFM 700195 (SB)**

Tw (°C)	Tf (°C)	output voltage (mV)	heat flux (kW/m <sup>2</sup> )
26.1	367.4	1.90	4.6
24.5	447.5	3.13	7.5
24.7	542.7	4.34	10.4
24.8	584.4	6.38	15.2
24.7	645.3	8.44	20.1
24.3	721.9	11.70	27.8
25.8	804.0	16.28	38.3
25.9	865.4	20.44	47.8



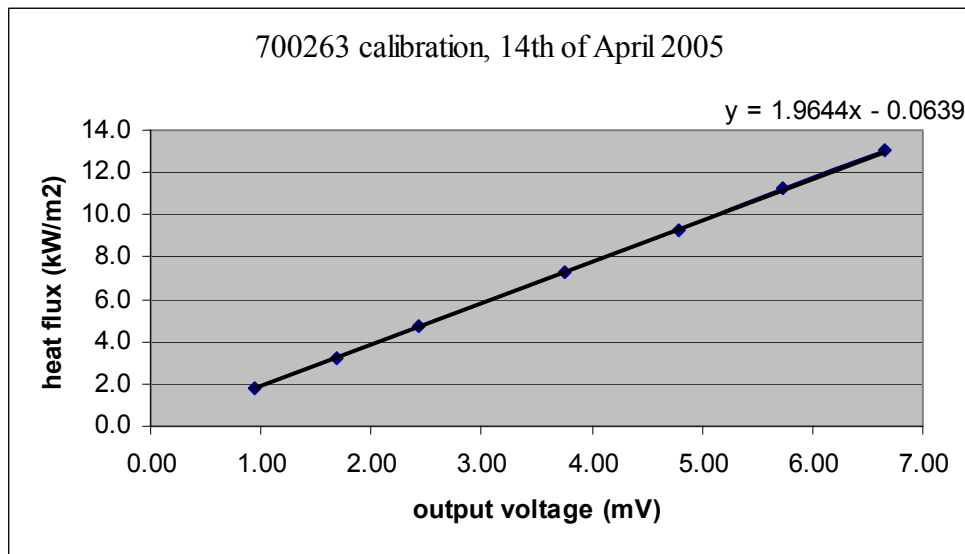
**HFM 700237 (SB)**

Tw (°C)	Tf (°C)	ouput voltage (mV)	heat flux (kW/m2)
25.2	367.2	1.90	4.6
25.0	447.6	3.09	7.5
24.8	507.6	4.30	10.4
25.3	584.6	6.30	15.3
25.1	645.5	8.33	20.2
25.5	721.5	11.60	27.9
25.3	761.9	13.60	32.7
25.2	804.0	15.94	38.4
25.1	836.1	17.91	43.2
25.3	865.5	19.87	48.0



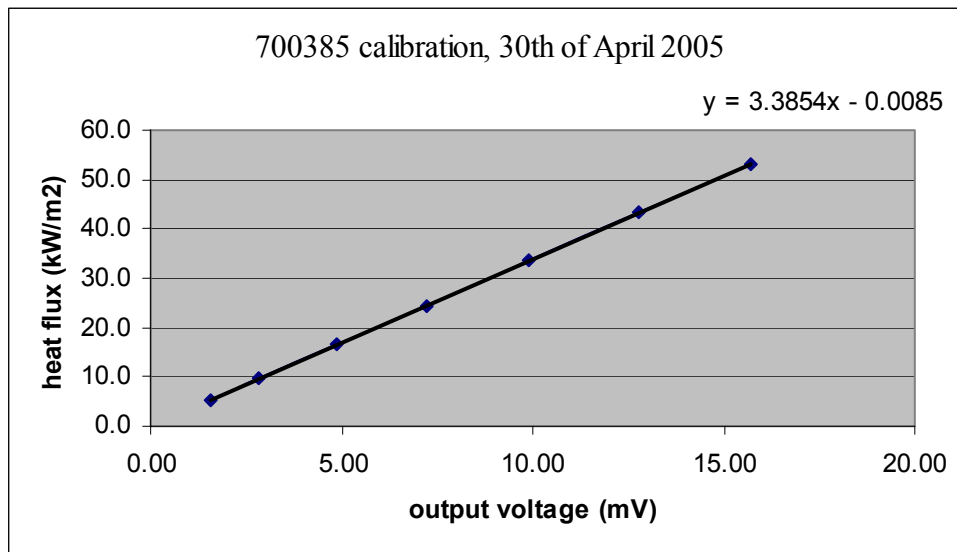
**HFM 700263 (SB)**

Tw (°C)	Tf (°C)	ouput voltage (mV)	heat flux (kW/m2)
26.2	406.7	0.94	1.8
25.6	510.5	1.69	3.3
25.7	584.5	2.44	4.7
25.4	681.8	3.76	7.3
25.7	740.3	4.78	9.3
26.0	790.0	5.74	11.2
25.9	830.3	6.65	13.0



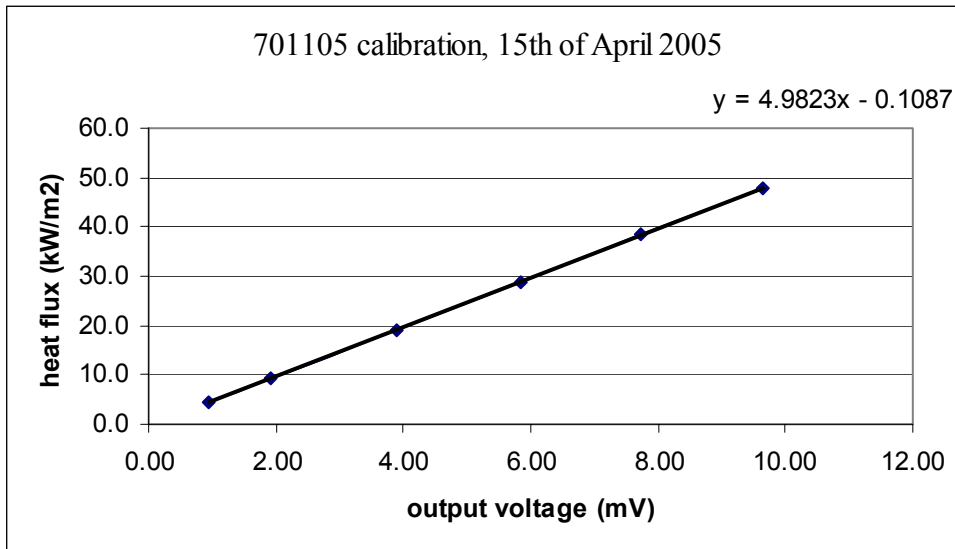
**HFM 700385 (SB)**

Tw (°C)	Tf (°C)	ouput voltage (mV)	heat flux (kW/m2)
25.9	391.9	1.59	5.4
25.8	491.5	2.83	9.6
25.8	601.4	4.88	16.5
25.9	690.5	7.23	24.5
25.8	768.6	9.90	33.5
25.8	836.8	12.77	43.3
25.9	895.2	15.71	53.2



**HFM 701105 (SB)**

Tw (°C)	Tf (°C)	ouput voltage (mV)	heat flux (kW/m2)
25.6	367.1	0.93	4.6
25.3	488.5	1.91	9.4
25.6	634.5	3.89	19.2
25.7	730.6	5.83	28.9
25.3	803.8	7.73	38.4
25.5	865.4	9.63	48.0



## Annex C Results of the comparisons

All calibrations performed before the 5<sup>th</sup> of May were performed with Imp5. Calibrations after that date were performed with an uncalibrated Imp borrowed from Solartron. A comparison performed with gauge 123731 (G) showed very similar results and therefore the borrowed Imp was not calibrated.

To calculate the difference, the last calibration is used as reference.

### HFM 123731 (G)

date	equation	q (kW/m <sup>2</sup> ) at u=10 mV	difference
3/26/2002	q=11.681u+0.9411	117.8	-0.1 %
4/28/2005	q=11.723u+0.6442	117.9	
7/5/2005	q=11.737u+0.6008	118.0	0.1 %

### HFM 123732 (SB)

date	equation	q (kW/m <sup>2</sup> ) at u=10 mV	difference
4/3/2002	q=12.539u+0.2056	125.6	1.0 %
5/2/2005	q=12.442u-0.05	124.4	

### HFM 701105 (SB)

date	equation	q (kW/m <sup>2</sup> ) at u=10 mV	difference
medtherm	q=5.025u	50.3	-1.1 %
2/5/2002	q=5.0295u+0.2686	50.6	-0.4 %
2/7/2002	q=5.021u+0.2430	50.5	-0.7 %
2/11/2002	q=5.0083u+0.2808	50.4	-0.8 %
2/13/2002	q=5.0245u+0.2212	50.5	-0.6 %
3/11/2002	q=5.0435u+0.0838	50.5	-0.5 %
3/12/2002	q=5.0256u+0.1984	50.5	-0.7 %
3/14/2002	q=5.0041u+0.2943	50.3	-0.9 %
2/19/2003	q=5.1008u+0.2980	51.3	1.0 %
4/28/2003	q=5.0478u+0.2411	50.7	-0.1 %
4/15/2005	q=4.9823u-0.1087	49.7	-2.2 %
7/9/2005	q=5.0862u-0.072	50.8	

### HFM 700263 (SB)

date	equation	q (kW/m <sup>2</sup> ) at u=10 mV	difference
medtherm	q=1.88u	18.8	-4.1 %
3/8/1995	q=1.9732u+0.0212	19.8	0.9 %
5/7/1996	q=1.9850u-0.02	19.8	1.3 %
8/24/1998	q=1.968u+0.0542	19.7	0.8 %
9/22/1999	q=1.9696u-0.0339	19.7	0.4 %
11/15/2000	q=1.9331u-0.0165	19.3	-1.4 %
11/7/2001	q=1.9758u+0.2311	20.0	2.0 %
12/11/2002	q=1.9446u+0.1866	19.6	0.3 %
4/13/2005	q=1.9644u-0.0639	19.6	

**HFM 700195 (SB)**

date	equation	q (kW/m <sup>2</sup> ) at u=10 mV	difference
medtherm	q=2.33u	23,3	-1,4 %
24/09/1993	q=2.3537u+0.9239	24,5	3,4 %
03/10/1994	q=2.4830u+0.1098	24,9	5,3 %
04/10/1995	q=2.4470u+0.1064	24,6	3,9 %
08/01/1997	q=2.4487u+0.0841	24,6	3,9 %
15/05/1998	q=2.4443u+0.0800	24,5	3,7 %
29/04/1999	q=2.4409u+0.0977	24,5	3,6 %
15/06/2000	q=2.3048u+0.0327	23,1	-2,4 %
25/09/2001	q=2.3553u+0.8111	24,4	3,0 %
10/09/2002	q=2.3551u+0.7872	24,3	2,9 %
20/02/2003	q=2.3970u+0.6655	24,6	4,1 %
25/04/2002	q=2.3596u+0.6884	24,3	2,7 %
28/08/2003	q=2.3673u+0.6815	24,4	3,0 %
28/08/2003	q=2.4035u+0.4896	24,5	3,7 %
27/01/2004	q=2.5451u+0.3857	25,8	8,6 %
13/04/2005	q=2.3345u+0.28	23,6	

**HFM 700237 (SB)**

date	equation	q (kW/m <sup>2</sup> ) at u=10 mV	difference
medtherm	q=2.31u	23.1	-4.5 %
11/11/1993	q=2.414u+0.038	24.2	0.2 %
10/4/1994	q=2.499u+0.049	25.0	3.6 %
10/4/1995	q=2.498u-0.1249	24.9	2.9 %
11/5/1996	q=2.502u+0.08	25.1	3.8 %
5/14/1998	q=2.4705u-0.0724	24.6	2.0 %
5/3/1999	q=2.4224u+0.0134	24.2	0.4 %
6/13/2000	q=2.3661u-0.2405	23.4	-3.1 %
9/27/2001	q=2.4072u+0.4865	24.6	1.7 %
9/12/2002	q=2.4297u+0.4083	24.7	2.3 %
9/11/2003	q=2.4429u+0.3035	24.7	2.4 %
9/11/2003	q=2.4279u+0.36	24.6	2.0 %
1/26/2004	q=2.5411u+0.1972	25.6	5.7 %
2/19/2004	q=2.5192u+0.0033	25.2	4.2 %
4/20/2005	q=2.4085u+0.052	24.1	

**HFM 700385 (SB)**

date	equation	q (kW/m <sup>2</sup> ) at u=10 mV	difference
2/24/1997	q=3.4884u+0.0129	34.9	3.0 %
10/23/2001	q=3.4262u+0.4136	34.7	2.4 %
4/30/2005	q=3.3854u-0.0085	33.8	

## Annex D One point calibration

### HFM 123731 (G)

point	equation $q=au+b$		heat flux (kW/m <sup>2</sup> ) at $u=5mV$	difference
	a	b		
all points	11.723	0.6442	59.3	
linear regression	11.88	0	59.4	0.24 %
1st point	12.286	0	61.4	3.53 %
2nd point	12.222	0	61.1	3.03 %
3rd point	12.145	0	60.7	2.41 %
4th point	12.046	0	60.2	1.61 %
5th point	11.973	0	59.9	1.01 %
6th point	11.9	0	59.5	0.40 %
7th point	11.861	0	59.3	0.08 %
8th point	11.84	0	59.2	-0.10 %
9th point	11.806	0	59.0	-0.39 %

### HFM 123732 (SB)

point	equation $q=au+b$		heat flux (kW/m <sup>2</sup> ) at $u=5mV$	difference
	a	b		
all points	12.442	-0.05	62.2	
linear regression	12.429	0	62.1	-0.02 %
1st point	12.429	0	62.1	-0.02 %
2nd point	12.424	0	62.1	-0.06 %
3rd point	12.419	0	62.1	-0.10 %
4th point	12.403	0	62.0	-0.23 %
5th point	12.407	0	62.0	-0.20 %
6th point	12.416	0	62.1	-0.13 %
7th point	12.425	0	62.1	-0.06 %
8th point	12.443	0	62.2	0.09 %
9th point	12.44	0	62.2	0.06 %

### HFM 700195 (SB)

point	equation $q=au+b$		heat flux (kW/m <sup>2</sup> ) at $u=5mV$	difference
	a	b		
all points	2.3345	0.28	12.0	
linear regression	2.3556	0	11.8	-1.48 %
1st point	2.4085	0	12.0	0.75 %
2nd point	2.3949	0	12.0	0.18 %
3rd point	2.3964	0	12.0	0.25 %
4th point	2.3895	0	11.9	-0.04 %
5th point	2.384	0	11.9	-0.27 %
6th point	2.3755	0	11.9	-0.63 %
7th point	2.3514	0	11.8	-1.66 %
8th point	2.3404	0	11.7	-2.14 %

**HFM 700237 (SB)**

point	equation $q=au+b$		heat flux (kW/m <sup>2</sup> ) at $u=5mV$	difference
	a	b		
all points	2.4085	0.052	12.1	
linear regression	2.4122	0	12.1	-0.28 %
1st point	2.4139	0	12.1	-0.21 %
2nd point	2.4295	0	12.1	0.44 %
3rd point	2.4279	0	12.1	0.37 %
4th point	2.4279	0	12.1	0.37 %
5th point	2.4248	0	12.1	0.24 %
6th point	2.4011	0	12.0	-0.74 %
7th point	2.4048	0	12.0	-0.59 %
8th point	2.4089	0	12.0	-0.42 %
9th point	2.4136	0	12.1	-0.22 %
10th point	2.4156	0	12.1	-0.14 %

**HFM 700263 (SB)**

point	equation $q=au+b$		heat flux (kW/m <sup>2</sup> ) at $u=5mV$	difference
	a	b		
all points	1.9644	-0.0639	9.8	
linear regression	1.951	0	9.8	-0.03 %
1st point	1.9339	0	9.7	-0.92 %
2nd point	1.9321	0	9.7	-1.01 %
3rd point	1.9343	0	9.7	-0.90 %
4th point	1.9374	0	9.7	-0.73 %
5th point	1.9377	0	9.7	-0.72 %
6th point	1.9571	0	9.8	0.28 %
7th point	1.9614	0	9.8	0.50 %

**HFM 700385 (SB)**

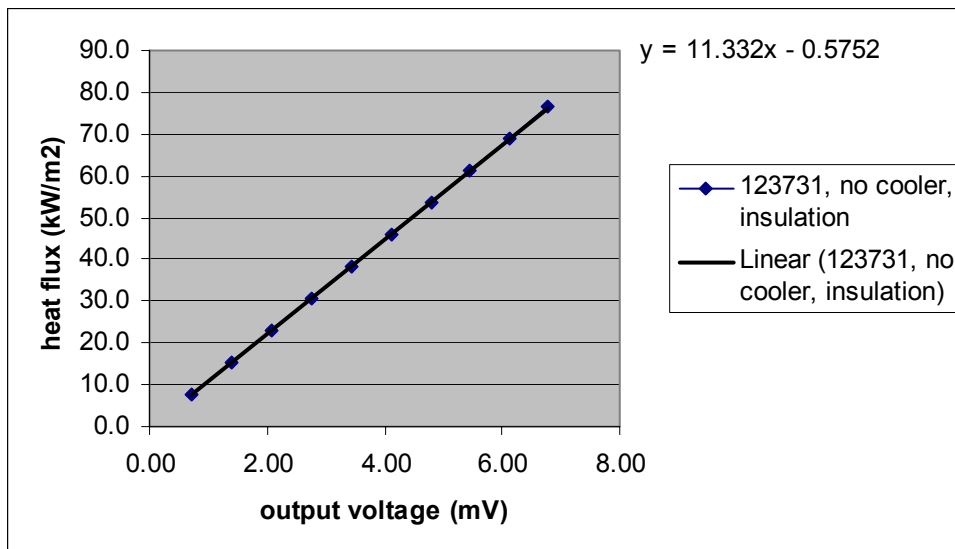
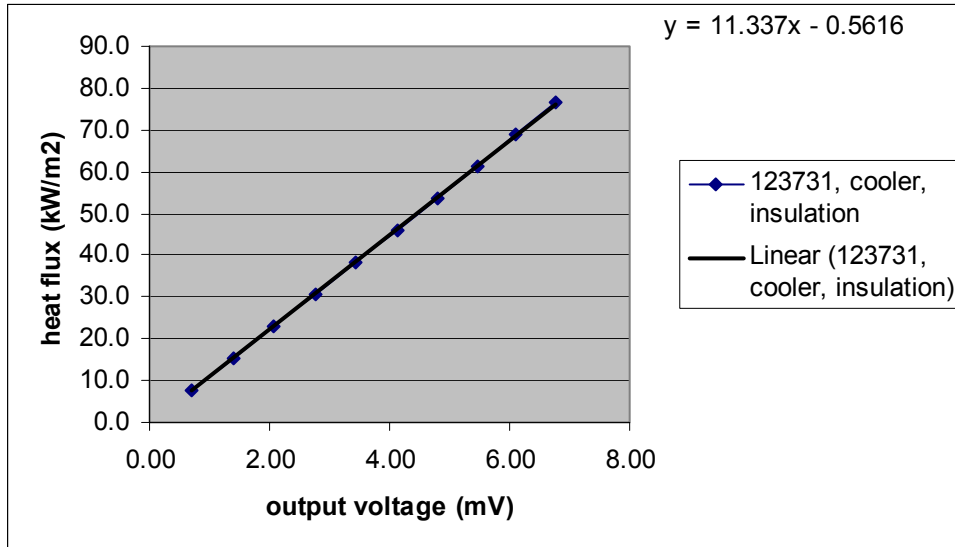
point	equation $q=au+b$		heat flux (kW/m <sup>2</sup> ) at $u=5mV$	difference
	a	b		
all points	3.3854	-0.0085	16.9	
linear regression	3.3846	0	16.9	0.03 %
1st point	3.3763	0	16.9	-0.22 %
2nd point	3.3786	0	16.9	-0.15 %
3rd point	3.3846	0	16.9	0.03 %
4th point	3.3857	0	16.9	0.06 %
5th point	3.3852	0	16.9	0.04 %
6th point	3.3856	0	16.9	0.06 %
7th point	3.3837	0	16.9	0.00 %

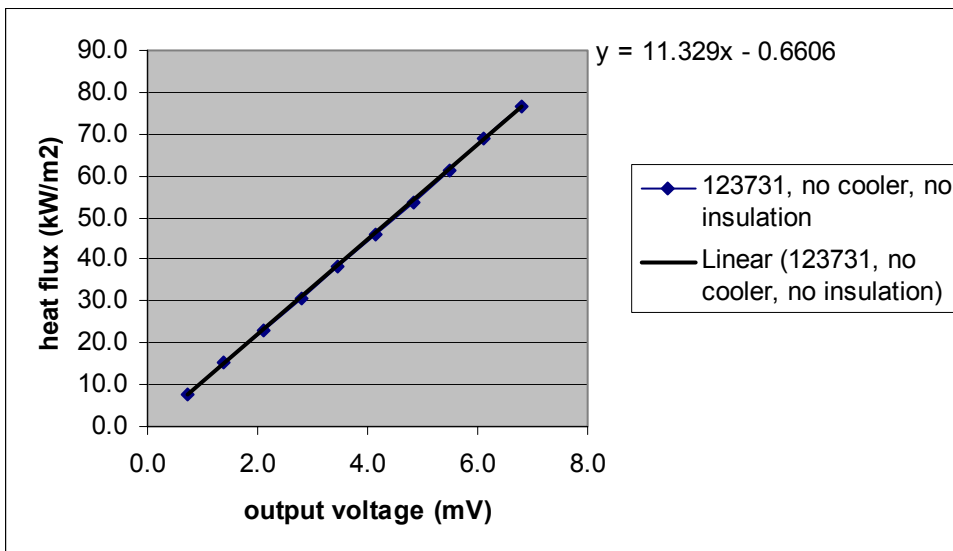
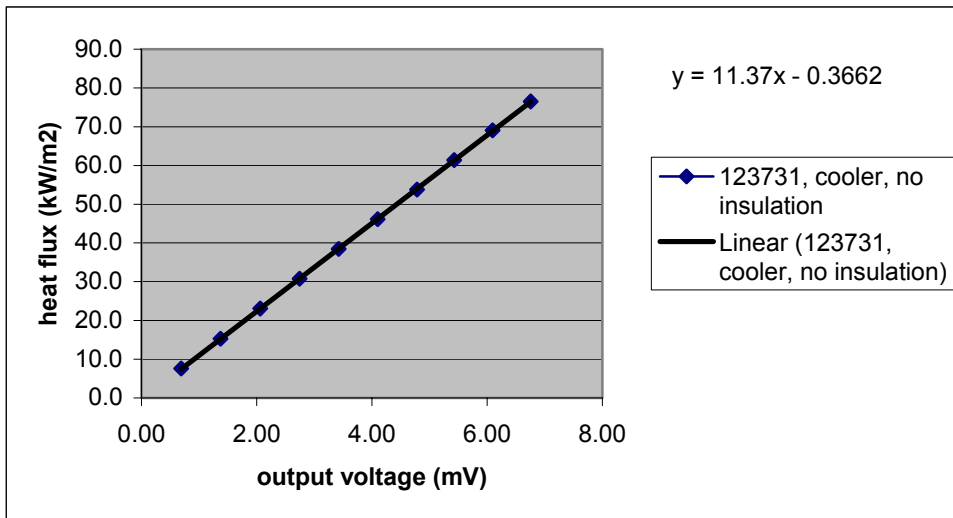
**HFM 701105 (SB)**

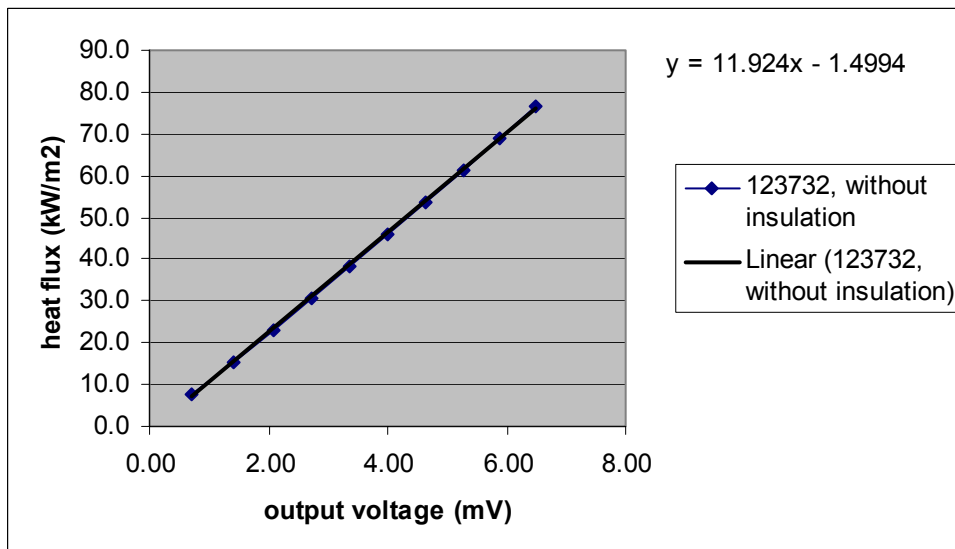
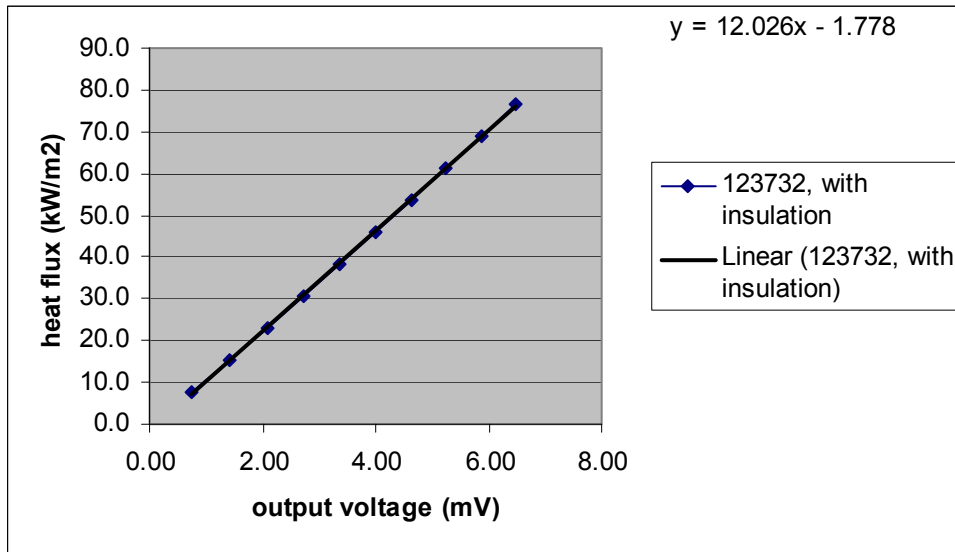
point	equation $q=au+b$		heat flux (kW/m <sup>2</sup> ) at $u=5mV$	difference
	a	b		
all points	4.9823	-0.1087	24.8	
linear regression	4.9666	0	24.8	0.12 %
1st point	4.9427	0	24.7	-0.36 %
2nd point	4.9202	0	24.6	-0.82 %
3rd point	4.9429	0	24.7	-0.36 %
4th point	4.9531	0	24.8	-0.15 %
5th point	4.9645	0	24.8	0.08 %
6th point	4.9787	0	24.9	0.36 %

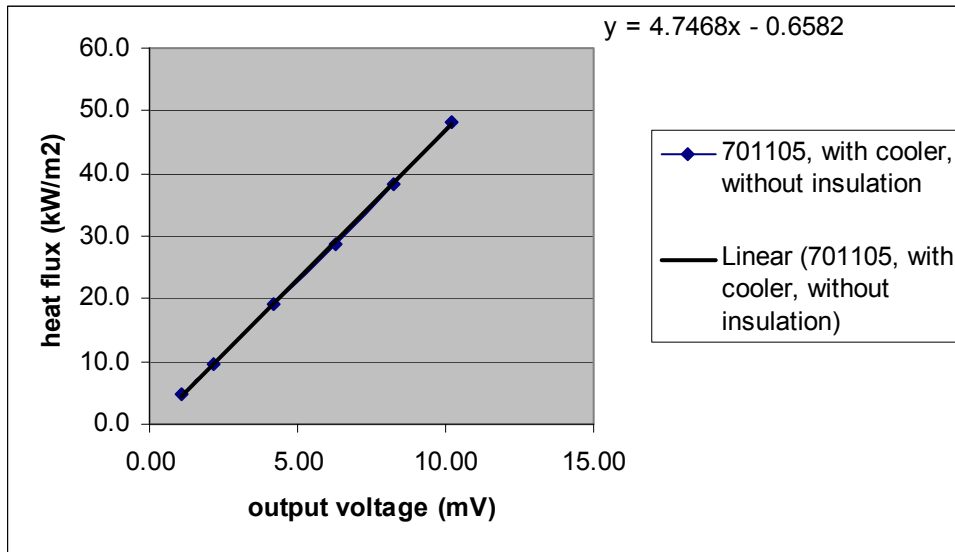
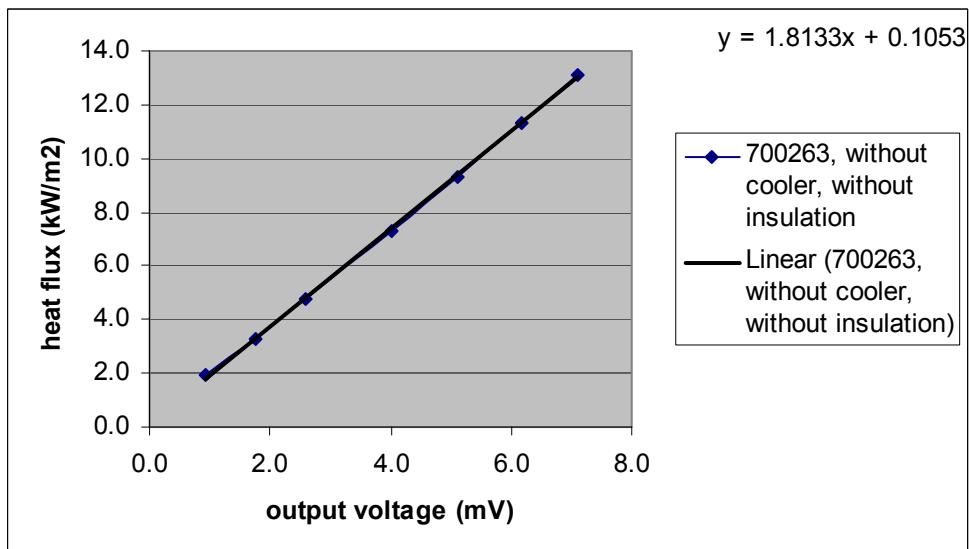
## Annex E Results of the calibrations, HFM flush with the wall

### HFM 123731 (G)





**HFM 123732 (SB)**

**HFM 701105 (SB)****HFM 700263 (SB)**

## Annex F Table thermocouple T

Celsius	mV	Celsius	mV	Celsius	mV	Celsius	mV	Celsius	mV
-100	-3.379	1	0.039	101	4.325	201	9.341	301	14.920
-99	-3.350	2	0.078	102	4.372	202	9.395	302	14.978
-98	-3.322	3	0.117	103	4.419	203	9.448	303	15.036
-97	-3.293	4	0.156	104	4.466	204	9.501	304	15.095
-96	-3.264	5	0.195	105	4.513	205	9.555	305	15.153
-95	-3.235	6	0.234	106	4.561	206	9.608	306	15.211
-94	-3.206	7	0.273	107	4.608	207	9.662	307	15.270
-93	-3.177	8	0.312	108	4.655	208	9.715	308	15.328
-92	-3.148	9	0.352	109	4.702	209	9.769	309	15.386
-91	-3.118	10	0.391	110	4.750	210	9.822	310	15.445
-90	-3.089	11	0.431	111	4.798	211	9.876	311	15.503
-89	-3.059	12	0.470	112	4.845	212	9.930	312	15.562
-88	-3.030	13	0.510	113	4.893	213	9.984	313	15.621
-87	-3.000	14	0.549	114	4.941	214	10.038	314	15.679
-86	-2.970	15	0.589	115	4.988	215	10.092	315	15.738
-85	-2.940	16	0.629	116	5.036	216	10.146	316	15.797
-84	-2.910	17	0.669	117	5.084	217	10.200	317	15.856
-83	-2.879	18	0.709	118	5.132	218	10.254	318	15.914
-82	-2.849	19	0.749	119	5.180	219	10.308	319	15.973
-81	-2.818	20	0.790	120	5.228	220	10.362	320	16.032
-80	-2.788	21	0.830	121	5.277	221	10.417	321	16.091
-79	-2.757	22	0.870	122	5.325	222	10.471	322	16.150
-78	-2.726	23	0.911	123	5.373	223	10.525	323	16.209
-77	-2.695	24	0.951	124	5.422	224	10.580	324	16.268
-76	-2.664	25	0.992	125	5.470	225	10.634	325	16.327
-75	-2.633	26	1.033	126	5.519	226	10.689	326	16.387
-74	-2.602	27	1.074	127	5.567	227	10.743	327	16.446
-73	-2.571	28	1.114	128	5.616	228	10.798	328	16.505
-72	-2.539	29	1.155	129	5.665	229	10.853	329	16.564
-71	-2.507	30	1.196	130	5.714	230	10.907	330	16.624
-70	-2.476	31	1.238	131	5.763	231	10.962	331	16.683
-69	-2.444	32	1.279	132	5.812	232	11.017	332	16.742
-68	-2.412	33	1.320	133	5.861	233	11.072	333	16.802
-67	-2.380	34	1.362	134	5.910	234	11.127	334	16.861
-66	-2.348	35	1.403	135	5.959	235	11.182	335	16.921
-65	-2.316	36	1.445	136	6.008	236	11.237	336	16.980
-64	-2.283	37	1.486	137	6.057	237	11.292	337	17.040
-63	-2.251	38	1.528	138	6.107	238	11.347	338	17.100
-62	-2.218	39	1.570	139	6.156	239	11.403	339	17.159
-61	-2.186	40	1.612	140	6.206	240	11.458	340	17.219
-60	-2.153	41	1.654	141	6.255	241	11.513	341	17.279
-59	-2.120	42	1.696	142	6.305	242	11.569	342	17.339
-58	-2.087	43	1.738	143	6.355	243	11.624	343	17.399
-57	-2.054	44	1.780	144	6.404	244	11.680	344	17.458
-56	-2.021	45	1.823	145	6.454	245	11.735	345	17.518
-55	-1.987	46	1.865	146	6.504	246	11.791	346	17.578
-54	-1.954	47	1.908	147	6.554	247	11.846	347	17.638
-53	-1.920	48	1.950	148	6.604	248	11.902	348	17.698
-52	-1.887	49	1.993	149	6.654	249	11.958	349	17.759
-51	-1.853	50	2.036	150	6.704	250	12.013	350	17.819
-50	-1.819	51	2.079	151	6.754	251	12.069		
-49	-1.785	52	2.122	152	6.805	252	12.125		
-48	-1.751	53	2.165	153	6.855	253	12.181		
-47	-1.717	54	2.208	154	6.905	254	12.237		
-46	-1.683	55	2.251	155	6.956	255	12.293		
-45	-1.648	56	2.294	156	7.006	256	12.349		
-44	-1.614	57	2.338	157	7.057	257	12.405		
-43	-1.579	58	2.381	158	7.107	258	12.461		
-42	-1.545	59	2.425	159	7.158	259	12.518		
-41	-1.510	60	2.468	160	7.209	260	12.574		
-40	-1.475	61	2.512	161	7.260	261	12.630		

-40	-1.475	61	2.512	161	7.260	261	12.630	
-39	-1.440	62	2.556	162	7.310	262	12.687	
-38	-1.405	63	2.600	163	7.361	263	12.743	
-37	-1.370	64	2.643	164	7.412	264	12.799	Thermometricscorp.com
-36	-1.335	65	2.687	165	7.463	265	12.856	
-35	-1.299	66	2.732	166	7.515	266	12.912	
-34	-1.264	67	2.776	167	7.566	267	12.969	
-33	-1.228	68	2.820	168	7.617	268	13.026	
-32	-1.192	69	2.864	169	7.668	269	13.082	
-31	-1.157	70	2.909	170	7.720	270	13.139	
-30	-1.121	71	2.953	171	7.771	271	13.196	
-29	-1.085	72	2.998	172	7.823	272	13.253	
-28	-1.049	73	3.043	173	7.874	273	13.310	
-27	-1.013	74	3.087	174	7.926	274	13.366	
-26	-0.976	75	3.132	175	7.977	275	13.423	
-25	-0.940	76	3.177	176	8.029	276	13.480	
-24	-0.904	77	3.222	177	8.081	277	13.537	
-23	-0.867	78	3.267	178	8.133	278	13.595	
-22	-0.830	79	3.312	179	8.185	279	13.652	Thermometricscorp.com
-21	-0.794	80	3.358	180	8.237	280	13.709	
-20	-0.757	81	3.403	181	8.289	281	13.766	
-19	-0.720	82	3.448	182	8.341	282	13.823	
-18	-0.683	83	3.494	183	8.393	283	13.881	
-17	-0.646	84	3.539	184	8.445	284	13.938	
-16	-0.608	85	3.585	185	8.497	285	13.995	
-15	-0.571	86	3.631	186	8.550	286	14.053	
-14	-0.534	87	3.677	187	8.602	287	14.110	
-13	-0.496	88	3.722	188	8.654	288	14.168	
-12	-0.459	89	3.768	189	8.707	289	14.226	
-11	-0.421	90	3.814	190	8.759	290	14.283	
-10	-0.383	91	3.860	191	8.812	291	14.341	
-9	-0.345	92	3.907	192	8.865	292	14.399	
-8	-0.307	93	3.953	193	8.917	293	14.456	
-7	-0.269	94	3.999	194	8.970	294	14.514	
-6	-0.231	95	4.046	195	9.023	295	14.572	
-5	-0.193	96	4.092	196	9.076	296	14.630	
-4	-0.154	97	4.138	197	9.129	297	14.688	
-3	-0.116	98	4.185	198	9.182	298	14.746	
-2	-0.077	99	4.232	199	9.235	299	14.804	
-1	-0.039	100	4.279	200	9.288	300	14.862	

SP Swedish National Testing and Research Institute develops and transfers technology for improving competitiveness and quality in industry, and for safety, conservation of resources and good environment in society as a whole. With Swedens widest and most sophisticated range of equipment and expertise for technical investigation, measurement, testing and certification, we perform research and development in close liaison with universities, institutes of technology and international partners.

SP is a EU-notified body and accredited test laboratory. Our headquarters are in Borås, in the west part of Sweden.



## SP Swedish National Testing and Research Institute

Box 857

SE-501 15 BORÅS, SWEDEN

Telephone: + 46 33 16 50 00, Telefax: +46 33 13 55 02

E-mail: [info.sp.se](mailto:info.sp.se), Internet: [www.sp.se](http://www.sp.se)

A Member of

 United Competence